Physical Basis of Scaling of Metabolic Rate with Organism Mass in Snowflake Yeast

Yash Rana

A dissertation submitted for the partial fulfilment
of BS-MS dual degree in Science

Indian Institute of Science Education and Research Mohali
April 2020

Certificate of Examination

This is to certify that the dissertation titled **"Physical Basis of Scaling of Metabolic Rate with Organism Mass in Snowflake Yeast"** submitted by **Yash Rana** (Reg. No. MS15042) for the partial fulfillment of BS-MS dual degree programme of the Institute, has been examined by the thesis committee duly appointed by the Institute. The committee finds the work done by the candidate satisfactory and recommends that the report be accepted.

Dr. Sanjeev Kumar Dr. Rajeev Kapri Dr. Abhishek Chaudhuri
(Supervisor)

Dated: June 10, 2020

Declaration

The work presented in this dissertation has been carried out by me under the guidance of Dr Abhishek Chaudhuri and Dr Shashi Thutupalli at the Indian Institute of Science Education and Research, Mohali and the Simons Centre for the Study of Living Machines, National Centre for Biological Sciences, Bangalore.

This work has not been submitted in part or in full for a degree, a diploma, or a fellowship to any other university or institute. Whenever contributions of others are involved, every effort is made to indicate this clearly, with due acknowledgement of collaborative research and discussions. This thesis is a bonafide record of original work done by me and all sources listed within have been detailed in the bibliography.

Yash Rana
(Candidate)

Dated: June 10, 2020

In my capacity as the internal supervisor of the candidate's project work, I certify that the above statements by the candidate are true to the best of my knowledge.

Dr. Abhishek Chaudhuri
Indian Institute of Science Education and Research, Mohali
(Internal Supervisor)

In my capacity as the external supervisor of the candidate's project work, I certify that the above statements by the candidate are true to the best of my knowledge.

Dr Shashi Thutupalli
Simons Centre for the Study of Living Machines
National Centre for Biological Sciences, Bangalore
(External Supervisor)

Acknowledgment

This thesis has served as a portal for my entry to a career in science. I will always cherish it as my first baby step into independent research.

My choice to study biological physics stem solely from my interactions with Dr. Abhishek Chaudhuri. He was the one who guided a 17 year old undergrad to journey through thermodynamics, to active matter to the origin of life to quantitative biological physics. He is by far the greatest teacher and mentor I have. Over the course of 5 years, he has imparted his wisdom of physics and taught me how to think about nature, molding me into the scientist I call myself today. I hope the future give me more opportunities to interact with him

Before working with Dr. Shashi Thutupalli, I was dead set to become a theoretical biophysicist. Working with him, made me realise how the progress of science hinges on great experimental discoveries. He has taught me how to ask the questions that offer insight and invite discussion. I hope that I can carry the same open-minded thinking, scientific rigour and refreshing enthusiasm that he possess as I journey into science. In the same breadth, I extend my heart-felt gratitude to Aditya Iyer, Nishant Narayanasamy, the members of the Thutupalli lab and Simon Centre for their guidance, teachings and care.

I would also like to thank my committee members, Dr. Rajeev Kapri and Dr. Sanjeev Kumar, for their helpful insights and comments and group members at IISER Mohali: Khusmeet, Misha, Nimisha, and Shubham Anand, for their friendship and acquaintance.

Over the last five years, I have had the pleasure of interacting with some amazing people, the MS15 Basketball team, SRC 2015, SRC 2017, iGEM 2018, the batch of MS15, the Ganapathy lab, the Bandopadhyay lab, the Feinerman lab, the Weber lab, the SCMP group and Dr.Sandeep Choubey. I owe them my sincerest gratitude.

A journey in science is at times one of solitude, but I am grateful to have with me my crew: Ankita, Shivansh, Vaibhav Kumar, Vaibhav Pal, Yateendra Sihag and Lt. Aneesha Maan who have taught me more than what is available in books and I will keep them with me like my skin for as long as I breathe.

Lastly, I thank my family, mom, dad and sister kirti, for their selfless love and care. Thank you for tolerating me for the past 22 years and those that come ahead.

-Yash Rana

Dedicated to Maa, Papa and my sister Kirti

List of Figures

Abstract

Scaling laws of physiological variables like life-span or metabolic rate with organism mass across biological species provide hint to underlying universal features of organisation in nature. One such law is the "Kleiber's Law" which is the observation that basal metabolic rate, B, is related to organismal mass, M, via the power law, $B \propto M^{\frac{3}{4}}$. The validity of such laws is often debated due to the noisy nature of data, absence of measurable parameters and lack of appropriate biological model organisms. In this thesis, we propose the use of a new model organism, Snowflake Yeast, a mutated strain of *Saccharomyces cerevisiae*, to test the validity of the Kleiber's law. Using microfluidics and isothermal calorimetry, we have arrived at data that seems to contradict the Kleiber's law. We also review the theoretical treatments to model the growth of the Snowflake and attempt to model its growth to explain the scaling relation.

Contents

Chapter 1

Introduction

1.1 Allometric scaling studies in Biology

Scaling is the study of how size leads to changes in biological traits. It teaches us how physical size constraints a physiological observable. For example, the study of heart rate across mammals (see figure 1.1). Historically, it has been studied using a power-law function of the following form:

$$Y = Y_0 M^b \tag{1.1}$$

Y : Physiological observable
M : Body mass of organism
b : Scaling exponent
Y_0 : Proportionality constant

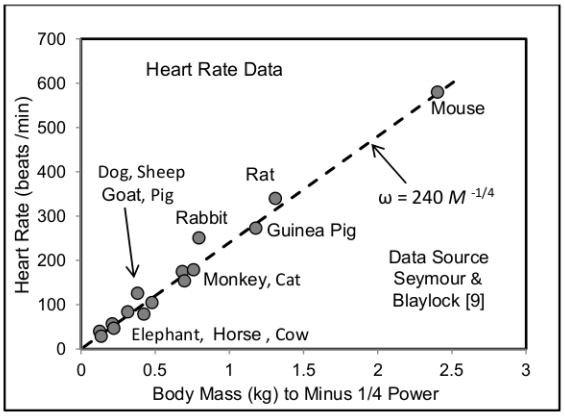

Figure 1.1: Allometric scaling of heart rate with body mass (taken from [14])

Of particular interest is the scaling exponent "b". When this exponent is not 1, the biological trait in consideration does not scale directly with mass, and the scaling of such traits is said to be allometric. It is an exciting branch which unites empirical studies, theories and experiments and has been used to study how numerous biological traits like heart rate, organ sizes, resource consumption vary with the body mass of organisms.

1.2 Metabolic Scaling studies

Amongst the various allometric studies, metabolic scaling is widely studied because it relates how energy production and consumption interact with size and growth (see figure 1.2). Furthermore, since products of metabolism related to biological function are acted upon by natural selection, it becomes interesting to study from an evolutionary perspective.

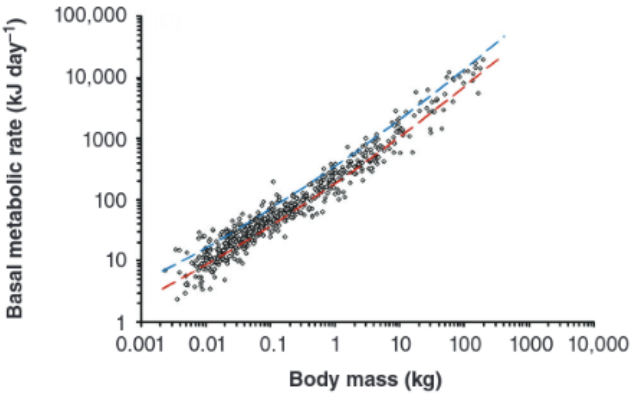

Figure 1.2: Consolidated data for Basal Metabolic Rate for mammals (taken from [47])

Several empirical studies have been carried out over the past 200 years, measuring metabolic activity by measuring heat production or using other proxies such as O_2 consumption and CO_2 production. Kleiber ([29],[28]) and others ([10],[6],[33]) reported that the scaling exponent for metabolic rate is close to 0.72 which gave birth to the **Kleiber's Law**, which is the observation that for a majority of organisms, metabolic rate scales to 3/4 power of the body mass of the organism.

1.2.1 What is the exponent of Metabolic Scaling in nature?

Since several allometric studies have concluded scaling exponents close to quarter-laws [43], it is debated that the scaling of metabolic rate may also obey a quarter law. Several articles also argue that this law is as fundamental as the Newton's laws of mechanics [39] and further debate is not warranted [43]. However, several empirical studies, meta-analysis studies and review articles disagree ([15],[48], [43], etc). The different and often exclusive ways of

choosing data points and the statistical tools used to analyse them lead to contradictory conclusions regarding the scaling exponent ([15], [48], [43]). In particular, for birds [15], the 3/4 exponent is rejected and for fishes [5] the scaling exponent varies between 0.5 to 1. The debate of the universality of quarter law exponents is not limited to metabolic scaling but also on other physiological parameters like respiration [39].

1.2.2 Theoretical treatments to study allometric scaling of metabolic rate

Several mechanistic and non-mechanistic theories have been proposed and reviewed to account for the allometric scaling of metabolic rate [19]:

- Surface area theories: These predict that heat dissipation should scale as the surface area of the organism since it is a mechanism for thermo-regulation ([42] and others).
- Resource distribution models: These models explain the observed scaling by the nature and constraints of the network which distribute nutrients to metabolising cells. ([46] and others)
- System-composition models: These models associate the allometric scaling to be related to the changes in relative contributions of components (organs or tissues) to the metabolic output of an organism with size ([22],[27].
- Resource-Demand Models: These models attribute the change in demand of resources for biological function (growth, locomotion and thermo-regulation) with size to the allometric scaling of metabolic rate [18].

There are theories that combine the above mechanism like the Dynamic energy budget theory (DEB), Metabolic-level boundaries hypothesis (MLBH) and the Contextual multimodal thoery (CMT). These theories have also been extended to create metabolic theories of ecology (MTEs) which try to explain ecological processes from individuals to ecosystems like population growth rate and trophic dynamics on the basis of metabolic scaling with body mass [7].

1.3 What is yet to be learnt?

The exact value of the scaling exponent might not be the most relevant quantity to debate over in the field of quantitative biology. Rather than be the Boltzmann, we need to be the Carnots or Clausiuses of our time and develop general principles that unify seemingly distinct features of biological systems. The need of the century is to identify more model systems amenable to experimental control ([44], [9]) which will give us quantitative data allowing us to differentiate between competing theories and make general statements in biology, in particular in the field of allometric scaling.

1.4 What is Snowflake Yeast?

The model organism used in this study is Snowflake yeast, a mutated strain of *Saccharomyces cerevisiae* which was experimentally evolved by Ratcliff et al. [37] by selecting for reduced settling time.

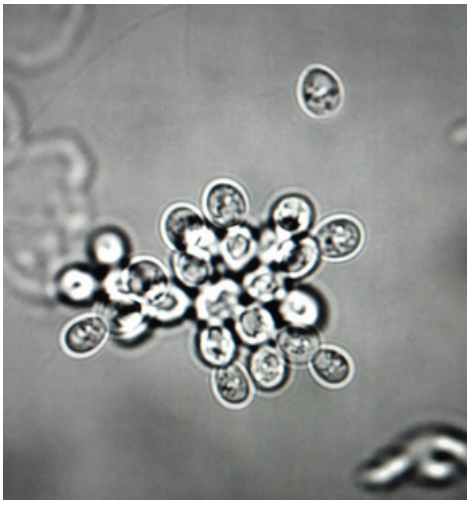

Figure 1.3: GOB2 Strain in media

Figure 1.3 shows an individual Snowflake yeast. It is composed of several yeast cells joined to each other at the point of budding. Since Snowflake yeast is a collection of several units of single cells, it is an excellent organism to study the change in metabolism with organism size.

1.4.1 Life cycle of wild type *Saccharomyces cerevisiae*

Wild type *Saccharomyces cerevisiae*, commonly known as baker's yeast are unicellular eukaryotic organisms which are round to ovoid ranging from $5 - 10\mu m$ in diameter. There are two forms of wild type yeast cells: haploid (with one complete set of chromosomes) and diploid (with two complete sets of chromosomes). The haploid cells have a mitosis life cycle depicted in figure 1.4 . It comprises of a long interphase (when the cell grows, and DNA content is doubled), prophase (when chromosomes condense, and the mitotic spindle is formed), prometaphase (when nuclear envelope vanishes and the microtubules of the spindle attach to the kinetochore), metaphase (when chromosomes align along the equatorial plane), anaphase (when daughter chromosomes are pulled apart), telophase (when nuclear envelope reforms) and end with cytokinesis when the bud is cut off from the parent cell. Diploids cells also follow a mitotic cycle; however, in conditions of stress, they can enter meiosis and form haploid spores which can later mate undergoing sexual reproduction.

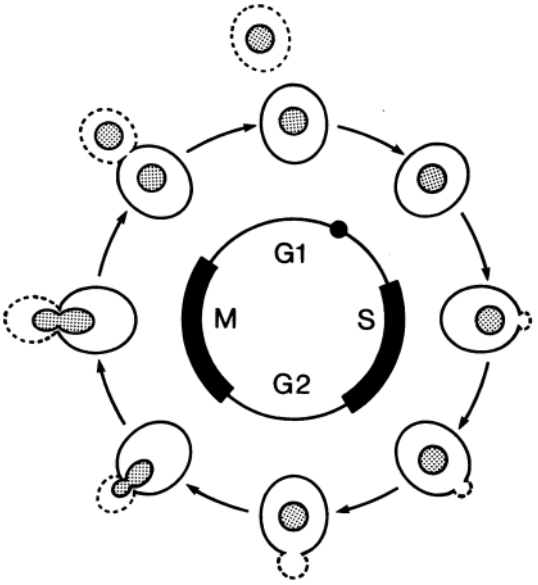

Figure 1.4: *Saccharomyces cerevisiae* mitotic life cycle with budding (taken from [23])

.

The duration of one cell doubling is roughly 100 mins at 30^0C [23]. This is an asexual form of reproduction which implies that the daughter cell and mother cell are genetically identical.

1.4.2 The origin of multicellularity

To understand the Snowflake yeast, one needs to understand and appreciate the experiment that displayed the experimental evolution of multicellularity using *Saccharomyces cerevisiae* [37]. The authors argue that the earliest form of multi-cellular organisms must have evolved from unicellular organisms capable of forming clusters after division (i.e. Post-divisional clusters). Post-divisional adhesion would reduce conflict of reproductive success within a cluster and would form the basis of highly differentiated complex multi-cellular organisms with elaborate labour division. They set up an evolution experiment which would favour cells that displayed the clustering phenotype (see figure 1.5). In gist, they allowed cultures of yeast (Wild type Y55) to grow overnight and enforced a gravity-based selection. They allowed the culture to stand for a certain amount of time (t_s, the settling time) and propagated a small fraction from the bottom of the flask. Organisms that made it to the bottom within the settling time survived the selection. If we consider the motion of a sphere in a fluid, the equation of motion would be the following:

$$\dot{v} = -(\frac{\rho_s - \rho_f}{\rho_s}) - (\frac{6\pi\eta a}{\rho_s V})v \tag{1.2}$$

$$\dot{v} = -\alpha - \beta v \tag{1.3}$$

where:
v : Instantaneous velocity of the sphere
ρ_s : Density of the sphere
ρ_f : Density of the fluid
η : Coefficient of viscosity
V : Volume of the sphere a : Cross-sectional area of the sphere
α : $(\frac{\rho_s - \rho_f}{\rho_s})$
β : $(\frac{6\pi\eta a}{\rho_s V})$ the solution for which is...

$$v(t) = -\frac{\alpha}{\beta}(1 - e^{-\beta t}) \tag{1.4}$$

Since $\frac{\alpha}{\beta} \propto R$, bigger clusters settle faster.

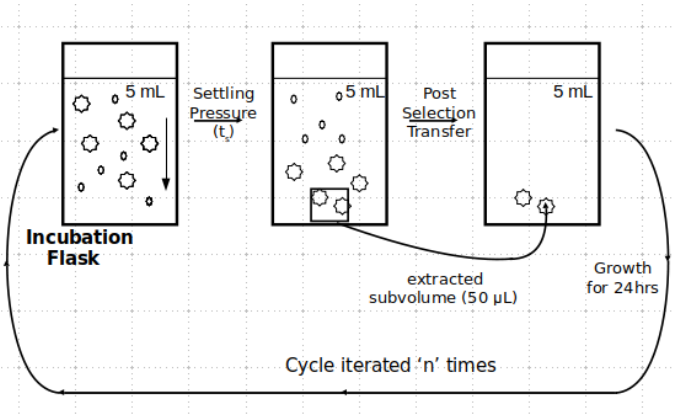

Figure 1.5: Schematic of experimental setup used in [37]

After 60 such selection rounds, the authors discovered that all replicates of the experiment displayed clustering phenotype. This experiment is important since it forms the starting point to create a range of distinct multi-cellular phenotype with variation in cluster size. which would allow us to check the validity of Kleiber's Law.

1.4.3 Snowflake yeast and its multi cellular life-cycle

If one tracks a single cell from the experimentally evolved population, as shown in figure 1.6, it grows from a single cell to a multi-cellular aggregate which then splits up into multiple clusters. The biggest size up to which a cluster grows is determined by the settling time used in the experimental protocol (t_S) [37]. The reproduction of phase of the multi-cellular organism, caused by the splitting of cluster, is hypothesised to arise from the breaking of weak links between the dead cells in the crowded interior of the cluster [38].The different stages of the multi-cellular life-cycle can be seen in figure 1.6.

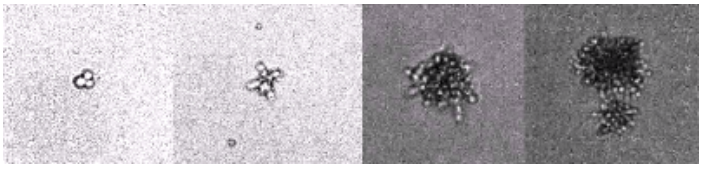

Figure 1.6: Life cycle of Snowflake Yeast (GOB 2 strain from Shashi Lab)

By tracking the growth of single snowflake, it is clear that all the cells in the cluster are exactly genetically identical as it forms via post-divisional adhesion and not the aggregation of genetically distinct cells (for example in biofilms). The cells enter mitosis but do not undergo cytokinesis, which is when the mother-daughter cell detach. The mother-daughter attachment site is visible by marking the bud-scar (the ring about which the mother and daughter cell are connected) with the chitin-binding marker calcofluor (see figure 1.7).

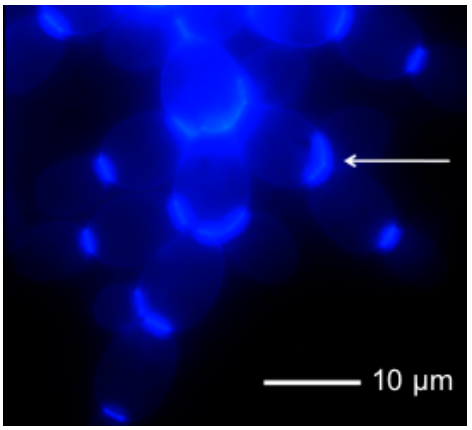

Figure 1.7: Calcofluor staining shows mother-daughter attachment sites. Taken from [37]
.

Upon investigation of the genome of the evolved population in comparison to the original wild type Y55 unicellular yeast, it was found that amongst 10 of the most down-regulated genes, seven are controlled by a single trans-acting transcription factor ACE2 [38]. Furthermore, these seven genes are directly involved in the degradation of the mother-daughter link, which explains the microscopy observations. The authors of [38] knocked out the gene responsible for the production of ACE2 and observed the clustering phenotype. By reintroducing, the gene synthetically, they were able to conclusively prove that a single gene could lead to the transition from unicellular to multi-cellular organisms. Understanding the genetic basis of the clustering phenotype teaches us that the growth of the Snowflake Yeast follows deterministic rules, to form well defined geometric structures. These rules will form the basis of our discussion in Chapter 4, where we model its growth.

1.5 Why is Snowflake Yeast a valid candidate to study the Kleiber's law?

By varying the setling time (t_S) used in experimental protocol by [37], we can generate populations of Snowflake yeast with different cluster sizes.The ability to manipulate the size of Snowflake yeast gives us an experimentally tractable system of populations with different characteristic masses.

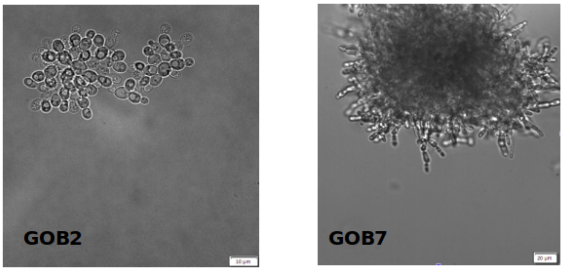

Figure 1.8: Size variation achieved using Snowflake Yeast

Figure 1.8 shows two of the seven Snowflake yeast populations maintained at the Thutupalli lab at NCBS, Bangalore. These populations can then be used to test the validity of Kleiber's law.

1.6 Plan of the thesis

In the second chapter of this thesis, we discuss the experiments to characterize the Snowflake Yeast. In the third chapter we measure it's metabolic activity using isothermal calorimetry and microfluidic experiments. In the fourth chapter, we discuss the various competing and contradictory models proposed to model the growth of the Snowflake Yeast and propose an independent model to do the same. Finally. In the fifth chapter we provide future directions and conclude.

Chapter 2

Experimental Characterisation of Snowflake Yeast

The Snowflake Yeast is a novel model organism. Therefore, to use it to study allometric scaling, it is important to firstly characterise the organism in terms of:

- Ideal conditions for maintaining populations
- Growth rate
- Mass of the organism
- Density of the organism
- Internal structure of Snowflake Yeast

2.1 Maintaining populations of Snowflake Yeast

The Snowflake yeast is an experimentally evolved population that has evolved in the extreme conditions of gravity selection. A tightly packed cluster of cells has limited access to nutrients (due to limited surface area) as opposed to a freely distributed population of the same cell type. The cells in a cluster can survive the gravity selection, but have limited access to resources due to their crowded surroundings. In the absence of the gravity selection unicellular yeast cells can grow faster and outnumber the clusters in a short period of time.Therefore, to avoid competition between unicellular yeast and the evolved population, we subject the Snowflake yeast to a round of gravity selection every 24 hours. The settling time used here is the same as that of the original experimental evolution experiment. The Snowflake yeast is incubated at 30^0C at 200 rpm in 5 mL falcon tubes containing glucose enriched YPD medium as described in table 2.1.

Reagent	Quantity
Yeast Extract	10 g
Peptone	20 g
Dextrose	20 g
Agar(for plating)	20 g

Table 2.1: Yeast Extract-Peptone-Dextrose (YPD) Medium [35]

2.1.1 Maintaining 7 populations based on settling time t_S

The Thutupalli lab at NCBS maintains seven distinct populations of Snowflake yeast. The populations are distinct for the settling time used in the daily gravity-based selection. The tuning of the strength of the gravity selection, by varying settling time has led to 6 orders of magnitude of mass variation amongst the different population. The daily transfer procedure is the following:

Step 1: Remove the falcon tube containing culture from the incubator and shake to homogenize the culture.

Step 2: Stand the falcon tube erect for the settling time t_S, shown in table 2.2.

Step 3: Extract 50 μL from the bottom of the falcon tube and transfer to a new falcon tube with 5 mL fresh media.

Step 4: Replace the new falcon tube into the incubator for 24 hrs.

Population ID	GOB3	GOB4	GOB5	GOB6	GOB7	GOB8
$t_S(min)$	2	1.5	1	30	*	*

Table 2.2: Settling time t_S for different populations (* Pick out the largest flake and transfer)

2.2 Age synchronization Study

The Snowflake yeast in media is a continuously growing organism. From a collection of single cells, individual clusters grow and reproduce to form more clusters. Since all cells do not divide simultaneously, there is a distribution of cluster sizes. Furthermore, once clusters start dividing, there is a vast spread in cluster sizes because of the simultaneous existence of juvenile, adult and reproducing Snowflake yeast. In this sense, any given population is "asynchronous" in terms of age (see figure 2.1).

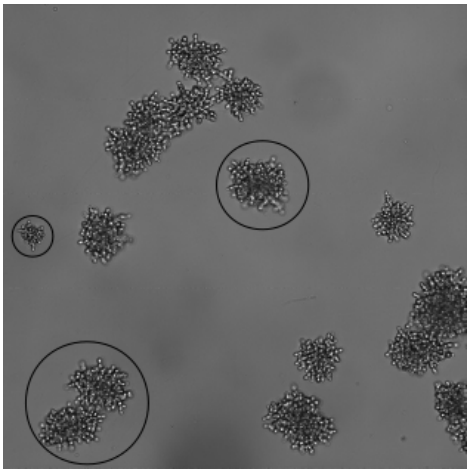

Figure 2.1: Asynchronous GOB3 population

Since one cannot conduct metabolic measurements of a single individual, we needed to find a method to generate populations of age synchronised individuals to get reliable data.

2.2.1 Chitinase digestion standardisation

The transcription factor ACE2, whose activity is disrupted in Snowflake yeast, regulates the genes responsible for mother-daughter separation [38]. One of the genes regulated by ACE2 is CTS1 which transcribes an endochitinase enzyme. Furthermore, the mother-daughter link contains the polymer chitin. Therefore, we proposed the use of enzyme Chitinase to deconstruct the Snowflake cluster into single cells (see figure 2.2). Another enzyme that can be used is lyticase [38]. However, since chitin is also a component of the cell wall of yeast cells, extensive chitinase treatment also leads to cell lysis.

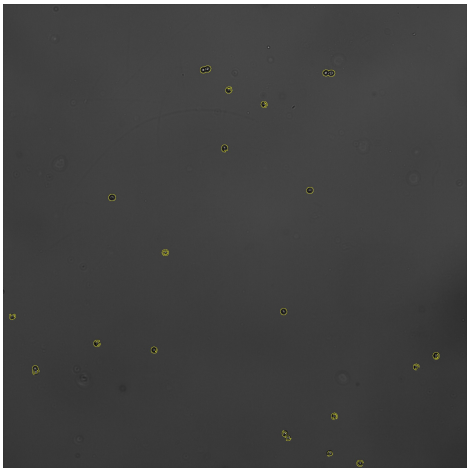

Figure 2.2: GOB2 after 12 hrs of 1mg/mL Chitinase digestion at 30^0 C at 300 rpm.

After numerous experiments by varying rpm, the concentration of the chitinase enzyme and duration for treatment for all the different population, we standardised the digestion treatment for all the Snowflake yeast populations. We found that we could use 1 mg/mL Chitinase at 300 rpm for all the populations by varying the duration of the digestion treatment.

2.2.2 Tracking synchronized populations

Once we were able to get single cells from clusters for the different population, it was important to track the synchronised growth of populations, to measure the duration up to which they remain synchronised. Once the cells start growing, the populations will remain synchronised until the clusters start reproducing and divide. This study not only tracked the life cycle of the Snowflake yeast but also gave us a time frame within which we could do ensemble metabolic measurements. To track the synchronised populations, we followed the following protocol (see figure 2.3):

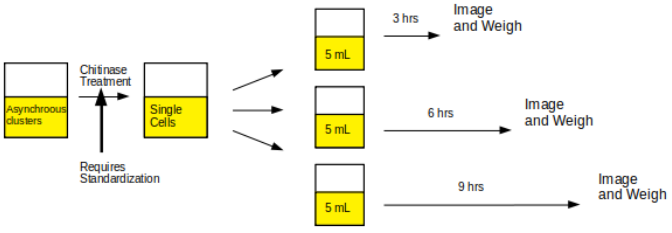

Figure 2.3: Schematic of experiment to track synchronised populations

Step 1: Digest asynchronous population with standardised chitinase treatment.

Step 2: Inoculate single cells in separate 5 mL flasks and incubate at 30^0C and 200 rpm.

Step 3: Remove flasks at different time points and image the Snowflake yeast to track growth.

Step 4: Repeat step 3 until total time from inoculation is 24 hrs

After experimenting on the different populations, we plotted the frequency distribution of the sizes of the cluster over time. We found that, for all the populations, the frequency distributions show the same qualitative features even though they are quantitatively different. As seen in Fig 2.4, in the beginning, the frequency distribution is uni-modal. With time, the spread increases due to initial conditions of individual cells and asynchronous cell division. After a particular time, the distribution becomes bi-modal because of the presence of a second population of Snowflakes. The second population is that of juvenile

Snowflake, formed from the reproduction adult Snowflake yeast. Beyond this time point, the frequency distribution spreads out, and we end up with an utterly asynchronous population of Snowflake yeast. The frequency distribution plot for the different time points may be plotted separately.

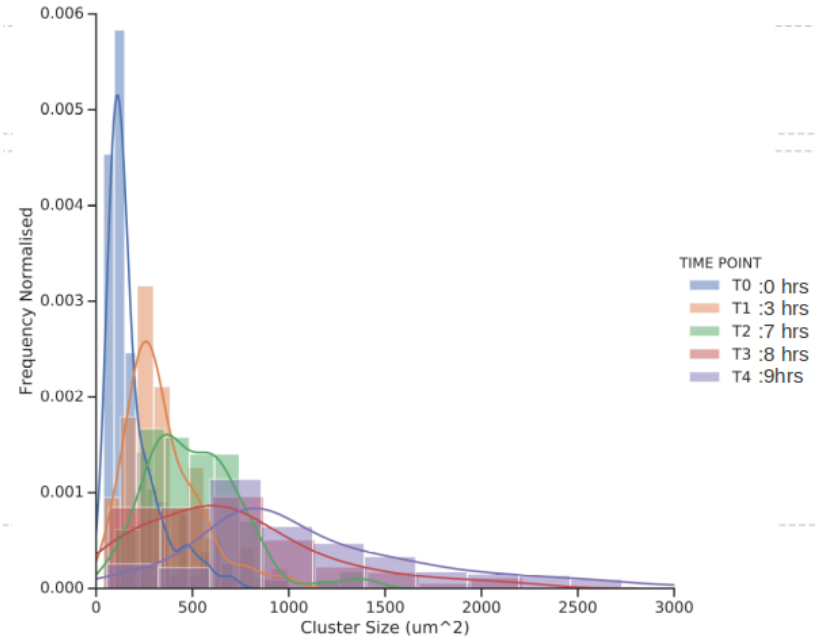

Figure 2.4: Frequency distribution for GOB2 population over time

As one can see in figure 2.5, at T2, 7 hrs from inoculation, the frequency distribution becomes bi-modal when individual Snowflake yeast start dividing as clusters. Any experiment, therefore, warranting synchronized GOB2 populations would have to be performed before this time point.

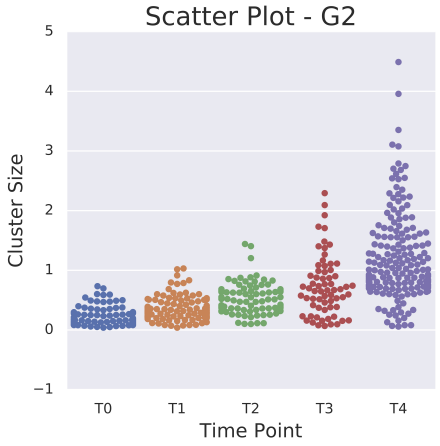

Figure 2.5: Scatter plot for size distribution of GOB2 population over time

2.3 Growth rate measurements of Snowflake yeast

The age synchronisation experiments described above allowed us to measure the growth rate of the Snowflake yeast. Figure 2.6 shows the raw data acquired at different time points of the age synchronisation experiment.

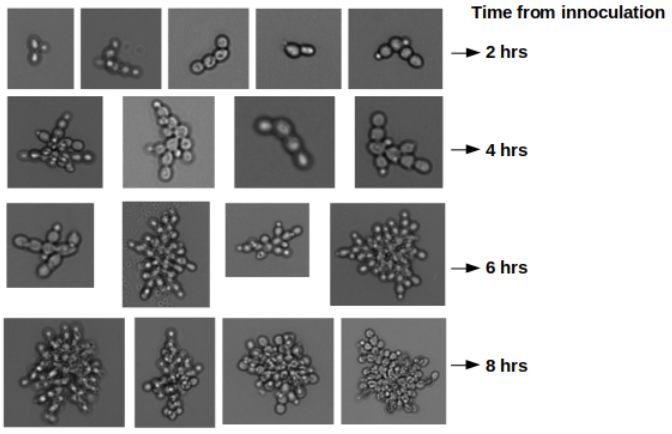

Figure 2.6: Individual Growth rate study of GOB3 population

2.3.1 Individual growth rate measurements

We used a macro on ImageJ to measure the areas of the clusters from the images acquired whilst tracking synchronised populations of Snowflake yeast. Figure 2.7 shows the growth curve of the different populations of Snowflake yeast. The plot shows variation in the growth rates of the different populations of Snowflake yeast. In particular,the growth rate of G2 population is lower than the rest. The growth curves of the other populations lie in the error bars of the other curves and hence are not quantitatively different.

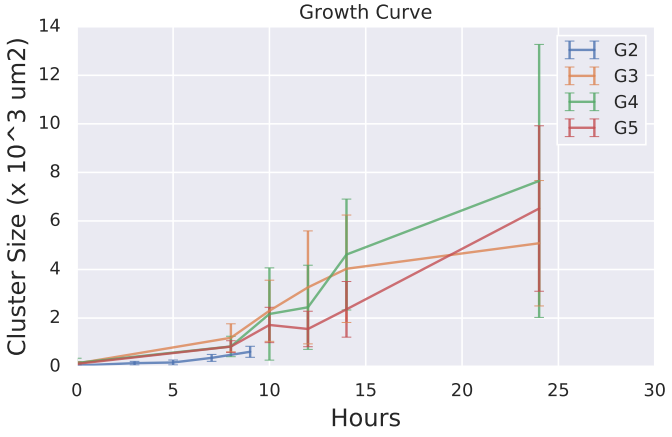

Figure 2.7: Individual Growth rates for different Snowflake yeast populations

It is also interesting to see the size of the cluster before they start dividing, as depicted in figure 2.8. As can be seen, the size at which the cluster divides is quantitatively different across the different populations. The size variation will allow us to conduct metabolic measurements across a range of organism mass.

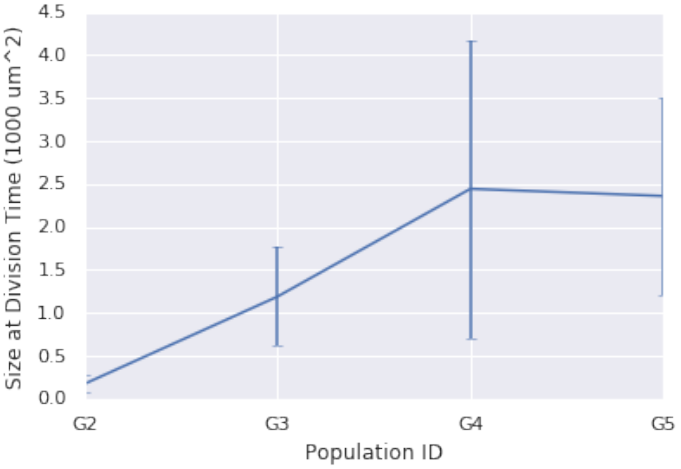

Figure 2.8: Cluster size at division for different Snowflake yeast populations

2.3.2 Population growth rate measurements

To measure population growth rates, we fashioned a chamber made from PDMS, which allowed us to image whole populations (see figure 2.9). We inoculated synchronised populations of Snowflake yeast and tracked the number of individuals to get an estimate of the population growth rate.

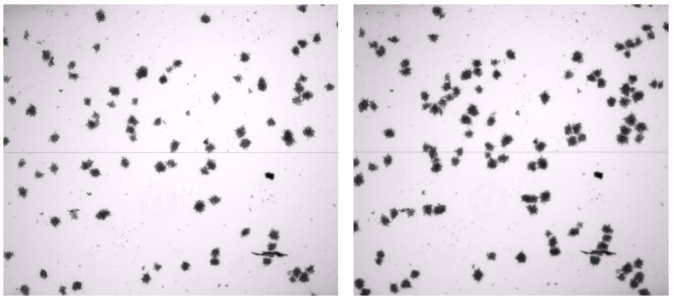

Figure 2.9: Images showing the doubling of GOB4 population

This allowed us to find the doubling times of the different populations of Snowflake yeast.

2.4 Calculating mass of Snowflake Yeast

A crucial physical parameter to measure in order to use the Snowflake yeast to verify the validity of Kleiber's law is its mass. Since the mass range of a single yeast cell is in the range of 2-4 pg ([**?**],[8]), measuring the mass of a Snowflake yeast is a tricky task. Several methods have been used to measure the mass of single yeast cells using suspended microchannel resonators(SMR)[8], measuring drag force on single yeast cells ([36],[21]) and cantilever-based micro-biosensors [30].

2.4.1 Wet mass measurement by volume displacement

Since these organisms exist in media, it is beneficial to measure the wet mass of the organism. Furthermore, any technique developed should not damage the organisms themselves while conducting the measurements. Keeping the above in mind, we developed the following measurement protocol depicted in figure 2.10:

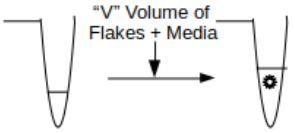

	Step 1	Step 2
Total volume of sample	V	2V
Total Volume of media	V	2V - δV
Total Mass	M_{media}	$2M_{media}$ - δM_{media} + M_{flake}

Figure 2.10: Technique to measure wet mass of Snowflake yeast

Step 1: Place a micro-centrifuge tube (MCT) on a weighing balance and re-scale the weight to zero.

Step 2: Pipette a volume 'V' of media into the MCT and weigh it.

Step 3: Pipette the same volume 'V' of culture into the MCT and weight it

Step 4: The difference in the weights is the mass of the Snowflake yeast with a systematic error coming due to missing volume of media.

A single yeast cell weighs in the range of *pgs*. Since a Snowflake contains hundreds of single cells and the innoculum would contain multiple Snowflakes, we expected the ensemble

mass to be in the range of μgs. However, this technique did not give reproducible results of ensemble mass, due to the following identified sources of error:

- Insertion of small volumes of media onto the weighing balance using micro-pipette incurs random error.
- Systematic error due to unaccounted volume of media.

This technique was used in the initial stages of the project, but due to its unreliability we searched for better techniques to measure mass.

2.4.2 Drag force experiment to calculate mass of single yeast cell

An exciting method to calculate the mass of the Snowflake yeast is to measure the mass of a single cell and use the number of cells in a Snowflake to estimate its total mass. This method involves the assumption that all cells have similar masses. To calculate the mass of a single cell, we decided to follow the protocol described by Rahman et al. [36] and developed a microfluidic device (Appendix B) to track the motion of single yeast cells along a channel.

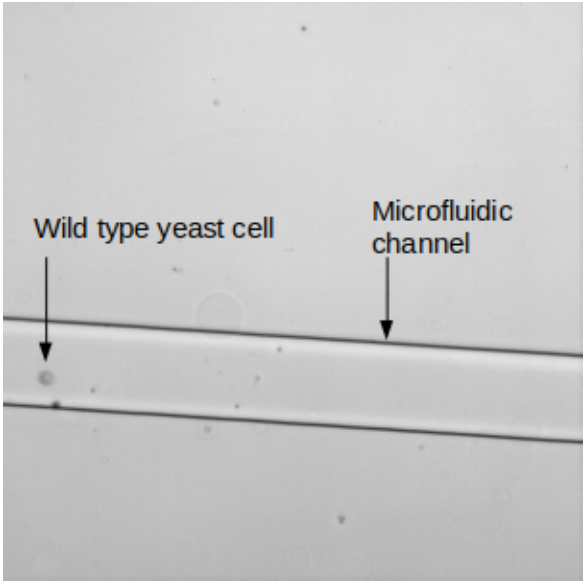

Figure 2.11: Drag force experiment to calculate mass of single yeast cell

We inserted wild type yeast cells on one end of the channel and attached the other end to a microfluidic pressure pump. We generated suction in order to induce motion of the cells. We then stopped the suction and tracked the deceleration of the yeast cells using an inverted microscope, as shown in figure 2.11. The drag force acting on a particle at high Reynolds number (> 1000) is [36] :

$$F_D = \frac{1}{2}\rho v^2 C_d A \tag{2.1}$$

where:
ρ = Density of the fluid
v = Speed of the object relative to the fluid
C_D = Drag coefficient
A : Cross sectional area

Balance of forces gives $ma = \frac{1}{2}\rho v^2 C_d A$ and when solved for the cell position with time gives us :

$$x(t) = \frac{1}{k}\ln\left(kv_0 t + 1\right) + x_0 \tag{2.2}$$

where $k = \frac{1}{2m}\rho v^2 C_d A$.

We tracked the position of the cell using image analysis and a tracking algorithm on MATLAB. By using the data of $x(t)$, we measured the quantity k. We could also extract the cross-sectional area using image analysis. Using the value of ρ of water and $C_D = 0.1$ [49], we arrived at the mass of a single cell to be $80pg$. Since this was an order of magnitude higher than previous measurements, we reviewed our experimental setup. We found that due to the existence of a background flow of fluid in the micro channel, we overestimated the relative velocity of the cell. The background flow led to an overestimation of mass. To correct for the background flow, we have planned to repeat the experiment with 0.5μ m tracer particles to measure the background flow to measure the relative velocity of the yeast cell to the medium.

2.4.3 Direct mass calculation by filter based mechanism

Since the mass of a single yeast cell is of the order of pg, the mass of a single Snowflake yeast cluster will be of the order of ng. A significant issue with measuring the mass of an ensemble is to extract a sufficient quantity of clusters from dilute cultures to get a measurable weight (μgs). Furthermore, it is not possible to extract biomass reliably beyond $2mL$ using centrifuging and pellet extraction. A possible technique is to pass culture through a filter paper and then drying the filter paper to measure the dry mass. Since there is no restriction on the amount of culture that can be passed through the filter paper, measurable weights can be achieved. This approach follows the glucose uptake kinetics study by Does et al. [16] and is a promising technique to measure the mass of Snowflake yeast in the future.

2.5 Calculating density of Snowflake Yeast

Calculating density is useful since it gives us a relationship between the mass and volume of the organism. Depending on which two quantities allow experimental access, the third one can be estimated.

2.5.1 Density gradient experiments using Percoll

Percoll can be used to create density gradients in the range of physiological densities [31]. Furthermore, its low osmolarity (= 20 mosM / kg H_2O) allows percoll solutions diluted with 1.5 M NaCl or 2.5 M sucrose to maintain the integrity of cells, viruses and even sub-cellular particles [12]. Percoll is a colloidal suspension of silica particles coated with PVP (polyvinyl pyrrolidone). Since there is a heterogeneity in the particle sizes, centrifugation causes the spontaneous formation of a density gradient. Alternatively, one can create a step gradient by stacking percoll bands of different densities on top of each other.

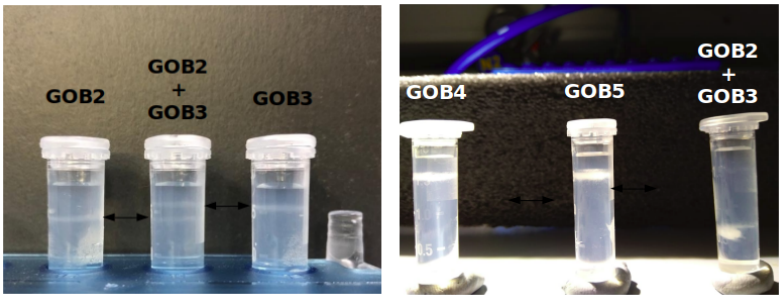

Figure 2.12: Percoll density gradient experiments with different density ranges.

Since the experimental evolution experiment selects for both density and volume, it is not surprising that the different populations have evolved different densities. A surprising result in figure 2.12 is that population GOB2 has a higher density than the other tested populations (GOB3, GOB4, GOB5). The above result is surprising and non-intuitive. Perhaps the volume increase in the other populations outweighs their low density. Once we have marker density bands, we will be able to quote the exact densities of the various populations. Since we have proof that the experimental evolution experiment has led to a change in cytoplasmic density, it will be exciting to see the mechanism of this variation. Genetic sequencing of the different populations may give us clues as to the control of density in these various populations.

2.6 Number of cells in a Snowflake

Across the evolution experiment, the size of the Snowflake yeast was observed to increase [37]. This increase is hypothesised by a change in an aspect ratio of the cells, which leads to

more efficient packing of cells [25]. To understand the increase in size and packing efficiency of Snowflake yeast, we needed to count the number of cells in a Snowflake.

2.6.1 Cell counting by plating

As seen in section "Chitinase digestion standardisation" it is, in principle, possible to digest a snowflake using a standardized chitinase treatment to get single cells. These cell suspension can be serially diluted and plated to get an estimate on the number of cells in a Snowflake. Unfortunately, experiments with GOB7 showed that there is a significant loss of cells during the chitinase treatment. This loss could be because the time required for the digestion of the interior of the cluster is sufficient for outer cells to lyse.

2.6.2 Cell counting by Flow cytometry

Once we get single cells by digesting the Snowflake yeast, we can also count the number of cells, using flow cytometry. The basic principle is that fluorescent detectors can detect cells passing through a laser beam in a single file. The detection can count and even sort cells. As the cell passes through the point of inspection, we record the forward scatter (FSC), and the side scatter (SSC) from detector placed parallel and perpendicular to the laser beam. The forward scatter can also be used to measure the cell volume (this provides an alternative strategy to calculate the total volume of the snowflake yeast)

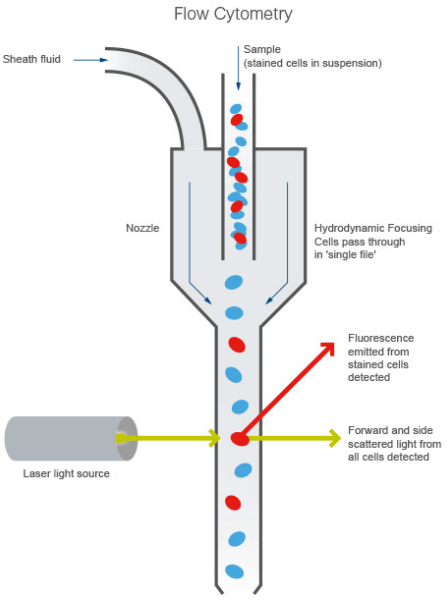

Figure 2.13: Schematic of Flow Cytometer (taken from [1])

Each cell passing through the laser beam results in a data point in the FSC vs SSC plot (see figure 2.14). Depending on the fluorescence intensity of dyes, we can also differentiate

between dead cells and live cells. By demarking regions in the plot for different types of cell (gating), we can count and sort cells.Its resourcefulness lies in the fact that over a 1000 cells can be scanned and sorted per second. This way, we can not only count the total number of cells in a Snowflake, but also comment on the heterogeneity of the Snowflake yeast.

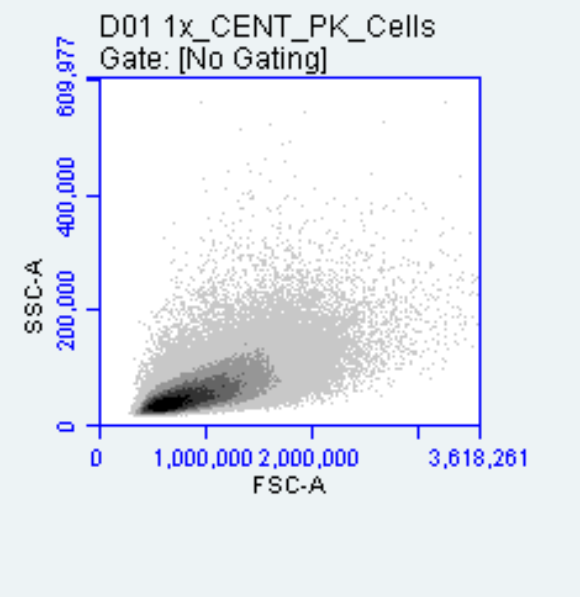

Figure 2.14: Flow cytometry data of Wild Type Cells

The above plot is the FSC vs SSC data of wild type yeast cells. We could count the yeast cells and found that there were 1538 cells / μL

2.7 Probing the internal structure of Snowflake Yeast

It is certain that the internal structure of the Snowflake yeast is heterogeneous [37]. Some cells are alive, some are apoptotic while the rest are dead as shown in figure 2.15.

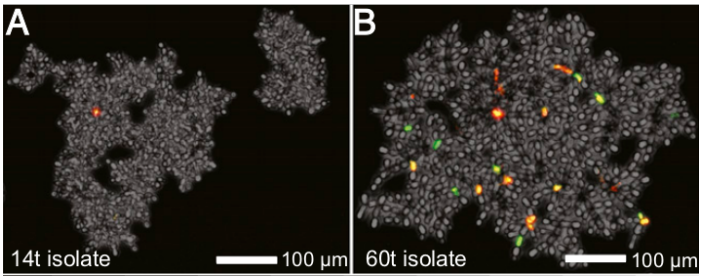

Figure 2.15: Heterogeneity amongst cells within a Snowflake(Dead cells are stained red (Propidium iodide), apoptotic cells are stained green (DHR)) [37]

This inspired us to look for experiments to understand the mysterious internal structure of the Snowflake yeast.

2.7.1 Testing the presence of resource allocation and distribution networks

Several theorists have tried to explain the origin of the apparent 3/4 allometric scaling law. West et al. [46] for instance, presented a model that predicted 3/4 power laws on the basis that nutrition distribution networks limit metabolism, and therefore, the structure of the resource distribution network governs the scaling law [46]. Such theories have inspired experimentalists [44] to search for empirical evidence for the origin of allometric scaling laws. During one of our experiments to measure growth rates of individual snowflakes, we observed bacterial contamination that showed flow patterns directed towards the centre of the Snowflake. To test the same in a controlled manner, we performed an experiment where we incubated the snowflakes with 0.5 μm sized red fluorescent protein-tagged micro-beads to confirm the presence of a directed flow (see figure 2.16).

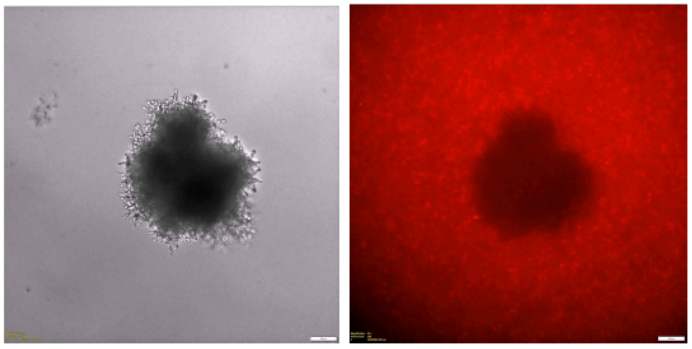

Figure 2.16: Experiment to test presence of directed flow towards Snowflakes

In the above experiment (figure 2.16), we incubated GOB7 Snowflake in 200 μL of YPD solution at 30^0C overnight and recorded using an inverted microscope at 0.2 fpm in the bright-field and RFP channel simultaneously. Qualitatively, it was seen that the micro-beads were being attracted to the Snowflake indicating flow of media towards the Snowflake.

2.7.2 Micro-injection experiments with Snowflake Yeast

After searching through literature, we found no evidence nor experiment claiming that there is an internal transfer of nutrients between cells of a single Snowflake. To test the above, we thought of a simple experiment: If we micro-inject GFP-tagged glucose into one of the cells and followed its motion through the snowflake, we would have conclusive evidence that a metabolite sharing amongst the cells of a snowflake. Metabolite sharing would indicate that the evolution of multicellularity might co-evolve with the evolution of nutrient distribution networks.

A literature review showed only one study which used a new shear based approach to micro-inject yeast [40], primarily because of its sturdy cell wall. Determined to try the

conventional method of micro-injection, we trained to perform micro-injection, received tutorial to use the needle puller and micro-tips from various labs at NCBS. We also received guidance from the micro-injection facility at InStem, NCBS.

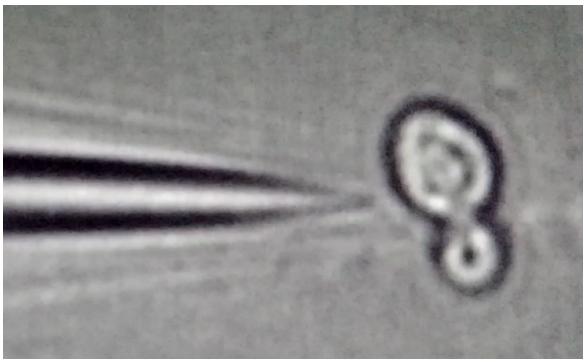

Figure 2.17: Micro-injection experiment to probe the internal structure of Snowflake Yeast

After receiving training, we tried to inject yeast with various substrates (see figure 2.17). Unfortunately, the sturdy cell wall of the yeast cell, prevented conventional micro-injection techniques (used to micro-inject embryos) to yield success. Our failed experiment also explained the lack of literature on yeast micro-injection.

2.7.3 Experiments with GFP-tagged glucose

To further test the internal structure of the Snowflake yeast, we performed an experiment where Snowflake yeast clusters were incubated with GFP-tagged glucose to see the differential uptake of glucose by cells within a single cluster.

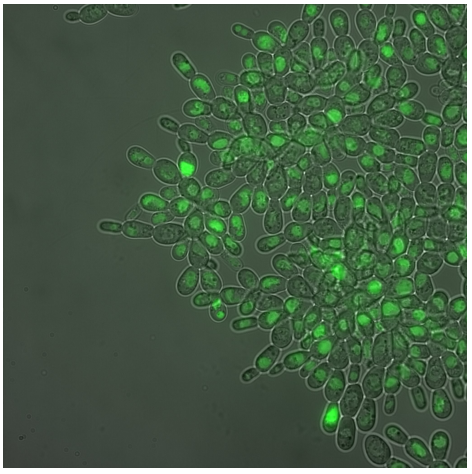

Figure 2.18: GOB4 incubated with GFP-tagged glucose

As one can see in figure 2.18, the amount of GFP glucose visible measured by the intensity of GFP is different in the different cells, indicating that the cells within the cluster

are heterogeneous, not only in terms of life status (being dead or alive), but also in terms of metabolic activity. This could also be indicative of the fact that all the cells are in different life stages. Therefore, the Snowflake yeast is truly a community of distinct cells forming an individual, making it a "Superorganism" [11].

Chapter 3

Metabolic measurements of Snowflake yeast

To comment on the allometric scaling of metabolic rate with organism mass using Snowflake yeast, we identified and measured proxies for metabolic activity. We chose to use the following two measures for metabolic activity:

- Heat exchange with the medium
- Glucose consumption rate

3.1 Isothermal titration Calorimetry

Isothermal titration calorimetry is a technique used to study a variety of physical processes. It can be used to study protein-ligand interaction, measure relative affinities and estimate stoichiometry of the interaction [34] and has also found use in studying RNA Biochemistry and Biophysics [17]. Furthermore, it has shown great application in studying embryonic development [41] and to measure heat dissipation of biological organisms as well [44]. Since heat dissipation is known to be a proxy to measure metabolic rate [26], we decided to use Isothermal titration calorimetry to estimate the metabolic activity of our model organism, Snowflake yeast.

3.1.1 Isothermal Titration Calorimeter

As depicted in figure 3.1, the instrument consists of two cells (or chambers). One is a reference cell, in which we add only the medium, while the other is the sample cell, where we add the medium with the Snowflake yeast. The instrument reads the change in temperature between the two cells and feeds this information back to compensate for any heat gain or loss in the sample cell in order to maintain the same temperature between the two cells.

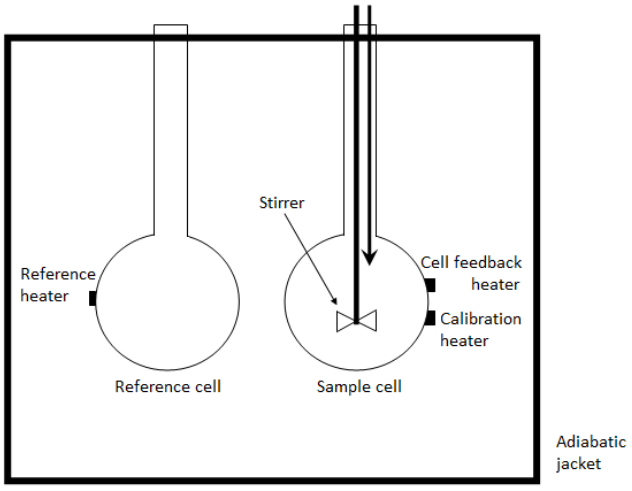

Figure 3.1: Schematic of the Isothermal Titration Calorimeter (taken from [2])

The protocol for a standard measurement is the following:

Step 1: Add $200\mu L$ of fresh glucose-enriched YPD media to both cells.

Step 2: Set the experimental temperature at 30^0C

Step 3: Allow ample time to allow the system to equilibrate to the experimental temperature. Equilibration is characterized by a (zero or non-zero) horizontal line on the heat flux graph.

Step 4: Remove $50\mu L$ of media from the sample cell and add $50\mu L$ of culture containing an age synchronized ensemble of Snowflake yeast.

Step 5: Wait for the heat flux graph to equilibrate at a new value.

Step 6: The difference in the two equilibrium value tells us the heat dissipation rate of the Snowflake.

3.1.2 Isothermal Calorimetry data

The calorimetry data is a time series of heat flux. The opening and closing of the calorimeter to insert the biological organism cause a transient spike in the time series, as shown in figure 3.2. The graph then settles to a new equilibrium value of heat flux which allows us to calculate the metabolic activity of the biological organism.

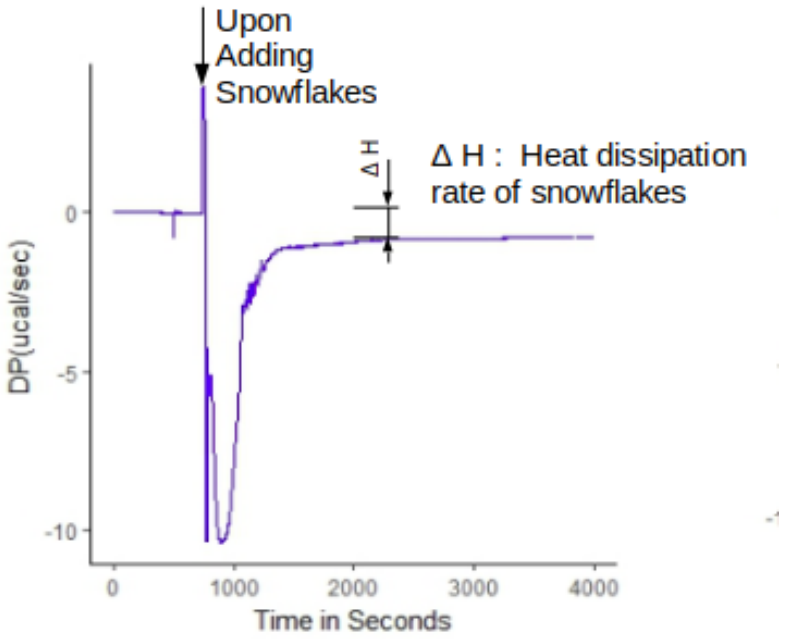

Figure 3.2: Isothermal Titration Calorimtery data for GOB7 population

3.1.3 Counter-intuitive results from failed experiments

Our initial experiments led us to a negative scaling exponent of metabolic rate with mass as shown in figure 3.3

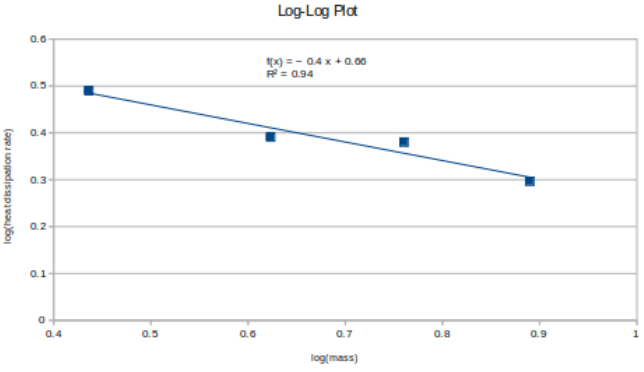

Figure 3.3: Counter intuitive result from failed experiments

We identified the following sources of error in our initial set of experiments:

- Experiments with asynchronous population of Snowflake yeast: Since the population were asynchronous, our calculated values for metabolic rate per individual were inconsistent and hence not reproducible.

- Large errors in mass measurement technique: Mass was measured using "Wet mass measurement by volume displacement" which as mentioned in Chapter 2 produced very high errors.

3.1.4 Revised experimental design

To overcome the sources of error as mentioned above, we decided to use standardisation mentioned in "Chitinase digestion standardisation" and adopt the following protocol, as shown in figure 3.4:

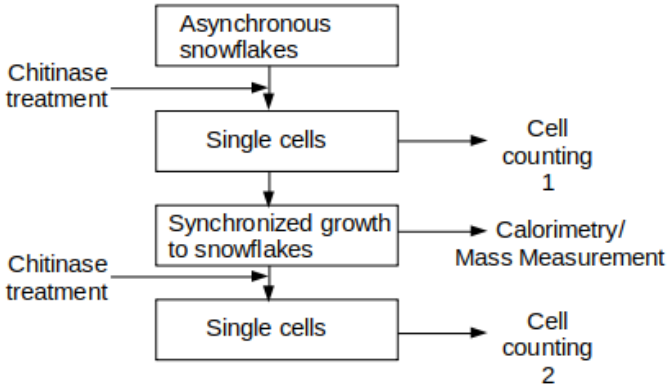

Figure 3.4: Flowchart for revised approach to be followed for calorimetry.

Step 1: Take an asynchronous population of Snowflake yeast and use the chitinase treatment to get single cells.

Step 2: Count a fixed fraction of cells to get the total cell density

Step 3: Let the Snowflake yeast grow till it reaches adult life stage.

Step 4: Use a fixed fraction of the synchronized population for calorimetry and the rest for mass measurement

Step 5: Use the chitinase treatment once again of synchronized populations. The digested cells can be counted to measure the number of cells in the adult Snowflake yeast.

Step 6: Repeat data collection for all populations of Snowflake yeast.

Upon following the above strategy and using the cross-sectional area as a measure of size, as opposed to mass, we were able to get clean data for wild type yeast, GOB2 and GOB4 populations as shown in figure 3.5:

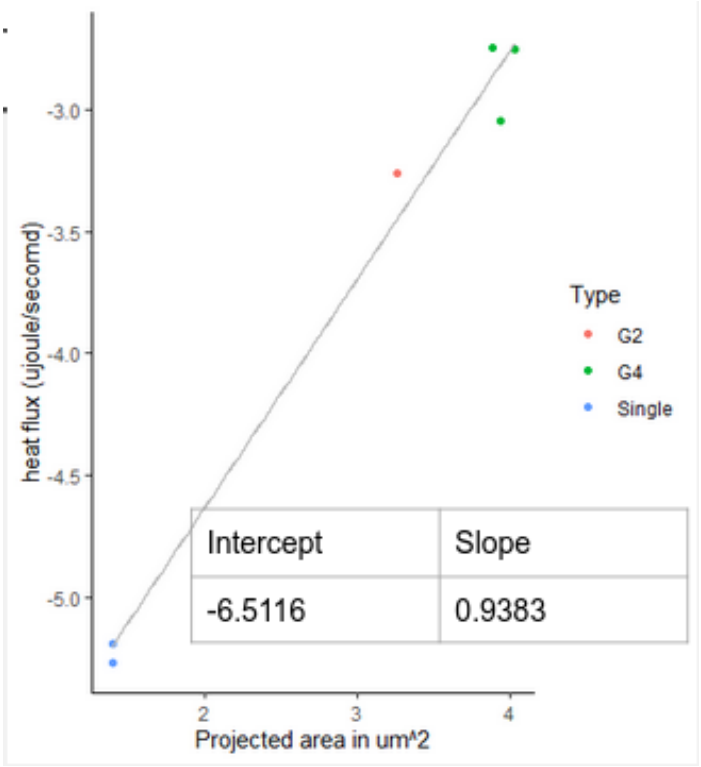

Figure 3.5: log-log plot of heat flux vs projected area

From the limited data we see a scaling that follows:

$$B \quad \alpha \quad A^{0.9383} \tag{3.1}$$

where:
B = Heat flux
A = Projected area
which implies,

$$B \quad \alpha \quad V^{\frac{2}{3}*0.9383} \quad \alpha \quad V^{0.6255} \quad \alpha \quad M^{0.6255} \tag{3.2}$$

where:
M = Organism mass
V = Organism volume

This value of scaling exponent should not be assumed to be the final value as the addition of more data points, and the correlation relation between the projected area and volume will change its value.

3.1.5 Evolution of cooperation between cells

Irrespective of whether the scaling exponent supports the existence of quarter-power laws in nature [43] or not; we can infer something insightful from the data presented. The mass of the Snowflake is the sum of the mass of the individual cells; however, the fact that the exponent measured is less than 1 (hypometric scaling) implies that the total metabolic activity is not the sum of the metabolic activity of the individual cells. Hypometric scaling indicates the metabolic cooperation between cells in a snowflake. It might also indicate that the evolution of multicellularity might also lead to the evolution of cooperation between cells in multi-cellular organisms.

3.2 Microfluidics experiments to measure glucose consumption

In past allometric studies, metabolic activity has been measure via direct calorimetry or indirect calorimetry using proxies like O_2 consumption or CO_2 production. Glucose consumption is also a valid measure of metabolic activity due to its direct utilization in energy production, see quation 3.3 [3].

$$C_6H_{12}O_6 + 2ADP + 2Pi \longrightarrow 2C_2H_5OH + 2CO_2 + 2ATP \tag{3.3}$$

To measure the same, we sought to employ the use of microfluidics. Microfluidic devices are analogous to Integrated circuits (ICs) of the silicon world in that they incorporate all functional components in a single space (see figure 3.6). Microfluidic technologies have been utilized in research and industry for multiple application like polymerase chain reactions (PCRs), drug screening and also single-cell studies [45]. Our primary aim was to develop microfluidic devices to develop an experimental setup to measure glucose consumption of Snowflake yeast trapped in droplets, inspired by [4]. Appendix B covers the method used to fabricate microfluidic devices.

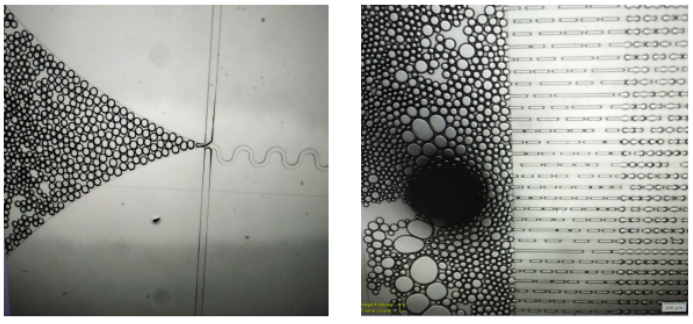

Figure 3.6: Microfluidic devices fabricated for the glucose consumption study.

3.2.1 Experimental design

Droplets of media containing Snowflake yeast suspended in an oil phase are used to create an inverse emulsion. The oil phase consists of mineral oil and a partially fluorinated alkane chain containing 0.75 % of a surfactant blend, adopted from [4]. When the Snowflake yeast consumes the nutrients present in the droplet, it creates an osmotic imbalance between droplets that contain the organism and those that do not. When droplets with an osmotic imbalance come into contact, the osmotic pressure is relaxed by the fastest diffusing molecule. A flow of water across the droplet boundaries causes a visible change in the volume of the droplets with can used to track the bio-activity of the Snowflake yeast. Volume reduction correlates with glucose consumption when the following conditions are met:

- The products of metabolism, CO_2, C_2H_5OH and ATP do not create an osmotic imabalance.
- Glucose cannot diffuse through the droplet boundary.

The first condition is met since CO_2 is soluble in oil; therefore, it diffuses faster than water or enters the continuous phase. Furthermore, C_2H_5OH has a solubility constant into the membrane one order of magnitude that of water [13] and hence its production does not lead to an osmotic imbalance. The second condition is met because the solubility constant of water in the membrane is two orders of magnitude that of glucose [13]. Therefore, any osmotic imbalance caused due to the consumption of glucose will be relaxed by diffusing water and not diffusing glucose. Once these conditions are met, the volume of the droplet should shrink as that for dilute solutions ($\mu \sim c$) governed by Fick's law:

$$\frac{dV}{dt} = -Fv_w\Delta c \tag{3.4}$$

where:
V : Volume of the drop
F : Transport factor reflecting membrane properties
v_w : molar volume of water
Δc : Time-dependent difference in glucose concentration

3.2.2 Test to check diffusion of glucose across droplet boundary

To check our system, we created a microfluidic device which could make droplets of two types in the same device. We used it to create droplets having different concentrations of glucose. Different colours of 0.5 μm fluorescent beads were used to distinguish between droplets with distinct contents. The qualitative result of the experiment is shown in figure 3.7:

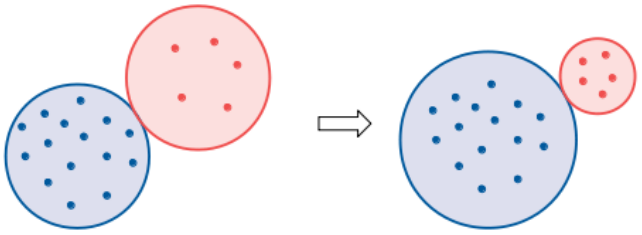

Figure 3.7: Test to check diffusion of water across droplet boundaries

As expected, there was an observable flux of water from the droplet having lower concentration of glucose to that containing higher concentration of glucose. This flux will theoretically stop when the osmotic pressure between the two droplets is the same.

3.2.3 Test to check diffusion of ethanol across droplet boundary

We used a microfluidic device to simultaneously create two types of droplets, one containing ethanol and one without ethanol. Different colours of 0.5 μm fluorescent beads were used to distinguish between droplets with distinct contents. The qualitative result is shown in figure 3.8:

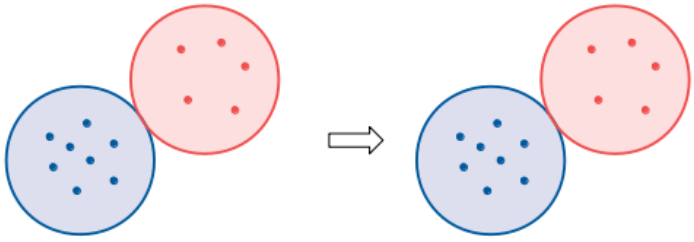

Figure 3.8: Test to check diffusion of ethanol across droplet boundaries

There was no observable change in the volumes of the droplets. No volume change indicates that the difference in ethanol within droplets does not lead to any exchange of water between droplets.

3.2.4 Measuring metabolic activity of Snowflake yeast

The next step was to trap individual snowflakes inside droplets containing media. After playing with the flow rates of the Snowflake yeast containing media and the immersion suspension, we were able to trap 20 μm GOB2 Snowflake yeast inside droplets. The expected setup for the final experiments is projected to be as shown in figure 3.9:

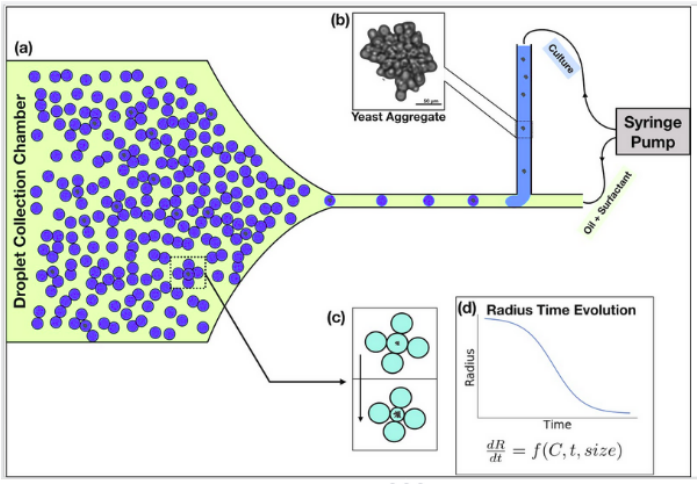

Figure 3.9: Experimental design to measure glucose consumption rate of Snowflake yeast.

A major advantage of such a setup is that we acquire data at the level of single individuals. This will not only allow us to get population information, required for allometry, but also the heterogeneity in metabolic activity amongst individual Snowflake yeast. Researchers at the Thutupalli lab have thereon proceeded to show that the volume of droplets containing Snowflake yeast indeed reduces in expectation with the proposed model of diffusion. At present, researchers at the Thutupalli lab have also developed a novel setup to track the exchange rate of materials from the medium of several isolated Snowflake yeast in parallel, truly harnessing the power of microfluidic devices.

Chapter 4

Modelling the Snowflake yeast

Models allow us to represent and explain the processes that underlie a process or physical phenomena. Building models help us comprehend data obtained from experiments or supplement data when experiments are not possible. In this sense, they try to form a link between theory and experiments. Models give us a starting point to think about physical phenomena; their predictions can be tested, and consequently, a model can be evolved, corrected or rejected. They are at the heart of knowledge building and portray how scientific knowledge is tentative. To better understand the Snowflake yeast and allometric scaling of metabolic activity of Snowflake yeast, we researched models available in the literature and sought to build one of our own.

4.1 Considerations while modeling the Snowflake Yeast

- *Tree structure*: The nature of the growth of Snowflake yeast leads to an unmistakable tree pattern.
- *Growth constraints*: Since the number of cells can potentially double in a cluster every reproductive cycle, it is not difficult to imagine that the geometry of the Snowflake yeast imposes severe restrictions on the nutrients supply and the volume available for the growth of cells.
- *Apoptosis*: The artificial selection imposed on the Snowflake yeast favoured high rates of cell death. [37]. Dead cells are hypothesized to be involved in the reproduction of the Snowflake yeast ([32],[37]).
- *Physical strain*: The volume constraint imposes compression strain on the budding cells. Physical strain is also credited in the reproduction of Snowflake yeast ([25],[32],[37]). Physical strain and cell death are both critical in determining when and where the cluster divides.

4.2 Review of previous models

Since the Snowflake yeast is a novel organism with a unique 3-D geometry, it is amenable to several theoretical treatments, and several researchers have attempted to do the same. Models suggested which do not recognize the geometrical arrangements of cells in the Snowflake yeast. However, they fail to explain the observations seen in the experimental evolution of Snowflake yeast. For example, they fail to explain why the rate of apoptosis increases with the size of the Snowflake yeast.

4.2.1 Modelling developmental pattern [38]

If all cells in a cluster reproduce at the same time, the number of cells at a distance x from the central node after d doublings will $\binom{d}{x}$ following a Pascal's triangle [38]. By taking into account the assynchornous nature of cell divison within a cluster by a paremeter $s \in (0, 1)$, they derived the number of cells at a distance x from the central node after $d + 1$ doubling time to be:

$$c_d(x) + s\left(\begin{pmatrix} d+1 \\ x \end{pmatrix} - \begin{pmatrix} d \\ x \end{pmatrix}\right) \tag{4.1}$$

Ref. [38] also uses the structure of the Snowflake yeast to provide analytical proof for how the geometry of the tree pattern increases the probability for individual-level mutations to reflect at cluster level phenotype by forming clonal propagules, linking micro and macro-evolution

4.2.2 Agent-based tracking of cells [32]

This model considers cells to be spherical balls connected to daughter cells via links in a tree graph. The addition of a node represents the birth of a new cell, and the death is represented by an inability to add more nodes to it. There are several vital features/assumptions of this model:

- Since cell death may be age-related, cells do not begin to die before a certain amount of time has passed from their last reproduction.
- Since experiments suggest that each cell can support at most five links, there is imposed degree cap on the daughter cells a cell has.
- Physical strain on cells is calculated by comparing the number of cells in the various branches connected to them.

- It assumes that the Snowflake maximizes volume by maximally spreading out and cells occupy shells according to the number of links from the central node. The implies that daughter cells of cells in the shell $k = 1$ will be in the shell $k = 2$ at a distance $3r$ - $5r$ (see figure 4.1).

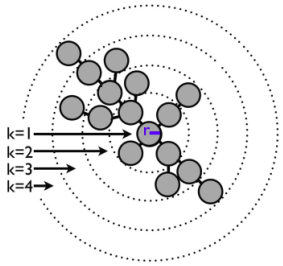

Generations (n)	Shells (k)					
	0	1	2	3	4	5
0	1	0	0	0	0	0
1	1	1	0	0	0	0
2	1	2	1	0	0	0
3	1	3	3	1	0	0
4	1	4	6	4	1	0
5	1	5	10	10	5	1

Figure 4.1: Shell arrangement used in model [32]

This gives us an easy way to calculate the number cells that can be present in any given shell:

$$\sum_{j=1}^{k} \begin{pmatrix} n \\ j \end{pmatrix} > (1+2k)^3 \tag{4.2}$$

Once this condition is reached, these cells are presumed to not reproduce any further.

- Once a cell dies, one of its links may get severed causing the reproduction of the cluster. The severance is biased by the sizes of the branches attached to it.

For each growth simulation, the rules of growth defined are:

Step 1: Start with a single node (Central cell)

Step 2: At each time step (doubling time), all the cells reproduce provided they are alive, have not yet reached a degree cap, below volume constraint defined by Eq 4.2

Step 3: At each time step, implement death based on the rate of apoptosis.

Step 4: If a cell dies, we break off one of its links to make a new individual.

Step 5: Note the tree structure after updating and go back to step 2.

This model gives insight on how cell death interacts with geometry within the multicellular yeast cluster. Interestingly, cell death opens up more space for new cells to grow, which counter-intuitively improve reproductive fitness. This model shows how geometry imposes constraints on biological function and fitness. Increased apoptosis could be selected for as it might increase cluster-level reproduction. Despite the insight provided by this model, it fails to account for the following:

- Compression strain due to budding cells.
- It also does not consider the fitness of cells based on the crowding of their local environment.

4.2.3 Geometric modelling of Snowflake growth [25]

AFM measurements show that the total compression force required to break a cluster is independent of cluster size [25]. These findings indicate that it is only essential for one link to break to cause reproduction of the cluster and that the inter-cellular bond strength is unchanged across the different size of Snowflake yeast. Furthermore, it is known that the aspect ratio of cells is larger for genotypes which produce larger cluster sizes [38]. This model tries to study the effect of the aspect ratio of cells in a cluster on the internal stress build-up due to volume constraints in Snowflake yeast. Key feature/ assumptions of the model are:

- Cells are assumed to be prolate spheroids (ellipsoids with equal "equatorial" radii) with aspect ratios taken from experimental observations.
- It assumes that yeast cells always bud at the opposite pole of their mother cell with a polar angle $45^0 \pm 10^0$.
- Cells may overlap, but the budding site can not. If a forbidden budding site is chosen, the cell skips reproduction for that reproductive cycle.
- The internal stress is calculated by estimating the linear overlap in volume between overlapping cells.

$$u_{ij} = (d - r_i - r_j)^2 \tag{4.3}$$

$$U = \sum_{i=1}^{N} \sum_{j \neq i}^{N} u_{ij} \tag{4.4}$$

  where:
  u_{ij} : Individual deformation energy
  d : Distance between centres of cells
  r_i : Equitorial distance of cell i
  U : Total deformation energy

- It uses an ad-hoc assumption for how many generations the cell reproduce: 12 (No clarification provided)

This model includes an important effect of considering the shapes of individual cells and the effect of the aspect ratio of the cells on the build-up of internal stress. This model proved

a causal relation between an increase in aspect ratio and the decrease in stress build-up in Snowflake yeast, giving rise to larger clusters. Despite the insight provided by this model, it does not take into account the following:

- This model does not take into account cell death and associates the reproduction of the cluster only as a consequence of building up of local internal stresses.
- It also does not comment on the dynamics of the growth, reproduction and size distribution of cluster before and after reproduction.

The same model is used in [24] to show that increasing aspect ratio to decrease internal stress build-up and delay inter-cell link severance is a better strategy than increasing inter-cell bond strength to increase the fitness of Snowflake yeast. The study highlights the importance of the elliptical shape and aspect ratio of cells in determining the stability of larger clusters. It also makes unsatisfactory alterations to the model in [25]:

- It takes away stochasticity in the choosing budding site. In particular, the outcome of a "magic angle" of packing in a cone is expected from the chosen rules of growth.
- It allows overlap between buds emerging from the same mother; this is not seen in experiments.
- It compares threshold stress and aspect ratio in limited parameter space, biasing results.

Other studies [**?**] have also discussed how reproductive specialization is favoured in tree-like sparse networks. These studies, however, do not comment on the growth dynamics of Snowflake yeast.

4.3 Proposed model for the growth of the Snowflake yeast

To incorporate the interaction of geometry, cell death and physical strain on the cells and study growth dynamics, we propose a new mechanistic model for the growth of the Snowflake yeast. Key features of the proposed model are:

- We incorporate the geometrical arrangement of cells by using a tree data structure with nodes representing cells and edges representing inter-cellular bonds.
- Cells are assumed to be prolate spheroids (ellipsoids with equal "equatorial" radii) with aspect ratios taken from experimental observations, inspired from [25]. Each cell is defined by its location, its orientation and its id on the tree data structure. This data is stored in the nodes of the data structure.

- We start with a single parent cell [32]. Cells reproduce normal to the surface of the ellipse, with a tunable volume overlap. Cells reproduce at an angle of $45^0 \pm 10^0$ [25] from the pole, forming a bud ring (see figure 4.2).
- Bud rings cannot overlap; if they do, the cell does not reproduce in that time step.
- Apoptosis is taken into account, and cells die (can be age-related as well). These cells do not reproduce and form weak links, where inter-cell bonds break.
- Internal stress on each inter-cell interaction is measured as in [24].
- Volume constraint is not accounted for as in [32]; however, cells stop reproducing when no more bud rings can be accommodated on the surface of the cell (biophysical degree cap).

The tree structure allows us to scan through the tree for neighbours. Furthermore, a reproduction event is dealt with as removing a sub-tree from the initial tree structure. The steps to study growth dynamics are similar to [32]; however we also track physical strain acting on each cell.

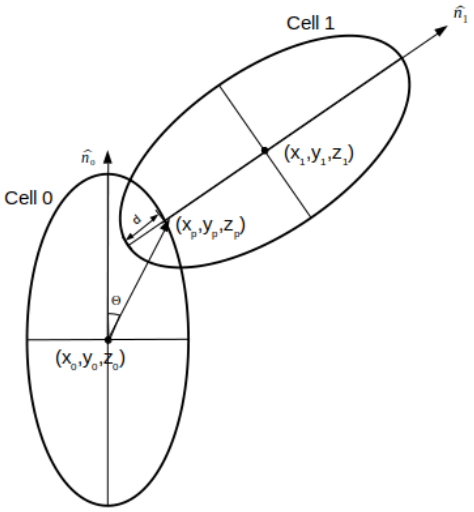

Figure 4.2: Geometric rules of growth of Snowflake in 3D

4.3.1 Hypotheses to test

The code is currently being built and tested, but we hope to test the following ideas:

- It might be the case that the physical strain determines when a cluster divides, but where the cluster divides depends on cell death.

- Such a model will also allow us to calculate strain on individual cells using a better quantitative measure than [32]. It will also allow us to see the differential strain across the cluster and help us understand the internal structure of the Snowflake yeast.
- Tracking the internal stress buildup can be used to track the life-cycle of a Snowflake yeast.
- We can also test the fitness of Snowflake yeast based on local crowding inside the cluster.
- Compare size distributions over time of Snowflake yeast growth with experimental observations.

We hope that this model gives a better understanding of the interplay between geometry, physical strain and cell death in Snowflake yeast. This model will give us insight into the structure and growth dynamics of Snowflake yeast.

Chapter 5

Conclusions and future plans

5.1 Concluding remarks

In this thesis, we have revisited the 200-year-old debate on allometric scaling laws in biology, in particular on the allometric scaling of metabolic rate with organism mass. We conclude that there is a grave need for manipulative quantitative experiments to differentiate between different theories of metabolic scaling. This task warrants the search for new and old model organism where one can achieve substantial range in size to conduct metabolic measurements. We propose the use of a novel experimentally evolved strain of *Saccharomyces cerevisiae*, Snowflake yeast, which forms tree-like multi-cellular structures with a tunable size giving access to 6 orders of magnitude of mass. We characterise the properties of this organism, like individual growth rate, population growth rate, number of cells, mass, density and internal heterogeneity using a variety of experimental techniques including microscopy, flow cytometry, micro-injection and microfluidics. We go on to make metabolic measurements of the Snowflake yeast using heat dissipation and glucose consumption as proxies. We do so using isothermal calorimetry and microfluidic experiments, respectively. We report the observation of a hypometric scaling suggesting the evolution of metabolic cooperation between individual cells in Snowflake yeast. Hypometric allometry also provides insight into the cooperation between cells as a consequence of the evolution of multicellularity. In the appendix, we discuss the engineering aspects of the thesis, namely construction of a wide field-of-view microscope and fabrication of microfluidic devices. In Chapter 4, we review models proposed to model the growth of the Snowflake yeast. We gather insights and discuss caveats in the models proposed. We go on to propose a novel model to study the interaction between geometry, physical stress and cell death in Snowflake yeast. This model will provide insight into the growth dynamics and internal structure of the Snowflake yeast.

5.2 Plans for the future

We aim to carry out the following tasks soon:

- More measurements of heat dissipation and glucose consumption to get statistically significant confidence in allometric scaling of metabolic rate in Snowflake yeast.
- Implement model proposed and compare with experimental observations of the growth and structural properties of Snowflake yeast.

Appendix A

Wide field-of-view(FOV) microscopy using flatbed scanner

Since studying population dynamics requires calculating numbers of individuals on a slide at the same time, being able to acquire a wide field-of-view image increases the accuracy of time points, reduces efforts and minimizes human error. Furthermore, wide field-of-view microscopy also helps in getting better statistics for other experiments studying individual snowflakes as well, for example, individual growth rates. To achieve high-throughput data acquisition for measuring growth curves of individual Snowflake yeasts and population dynamics, we decided to create a wide field-of-view microscope from scratch. This endeavour was inspired by work carried out by *Zheng et al* [50] and *Göröcs et al* [20].

A.1 Approach to build

Conventional microscopes are limited in field-of-view primarily because of limited spatial bandwidth product (a measure of the information contained in an image). This limitation implies that increasing the field-of-view will directly lead to a reduction in resolution. Therefore, to maintain resolution while increasing field-of-view, we need to increase the spatial bandwidth product of our image acquisition. Several ways can do this:

- Using multiple objectives for parallel imaging
- Hardware modification to implement slide scanning.
- Contact imaging microscopy etc

While several positive steps were also successful with regards to hardware modification to implement slide scanning, we also constructed our microscope from the schema proposed in [50], see figure A.1.

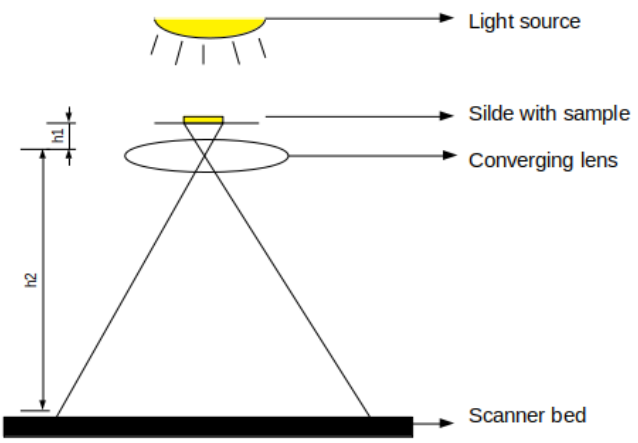

Figure A.1: Schematic for home-made wide field-of-view microscope

A.2 Construction of wide FOV microscope

We removed the camera and optical relay system from an old inverted microscope for a base, lens holder and light source. We removed the glass panel from a Canon CanoScan LiDE300 scanner and inserted on the base of the re-purposed microscope. We then used a spare condenser lens as the converging lens for our microscope and placed our slide with sample on top of the condenser lens (see figure A.2). To estimate the resolution achieved, for a 1 cm x 1 cm slide, with the lens adjusted to achieve a magnification of 30 x and the scanner set at 2400 x 2400 dpi, we can scan the whole slide at 0.34 μm resolution. To give a comparison, if we use green light (514 nm) to image a specimen with an oil immersion objection of the numerical aperture of 1.45, then the resolution would be 0.17 μm.

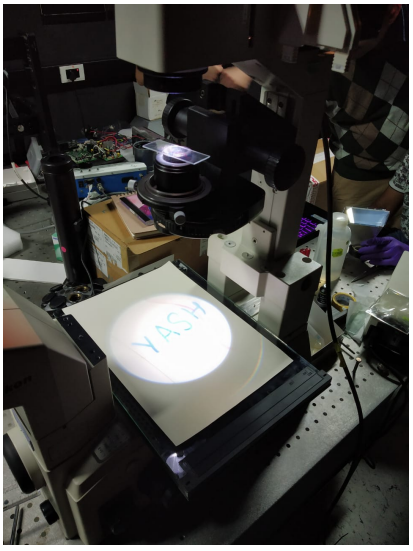

Figure A.2: Initial stages of home-made wide FOV microscope

Despite being able to construct the microscope, we faced several issues in regards to bypassing the Canon software (to scan on demand) and deactivating hardware components of the scanner without upsetting the software. However, since scanner technology seemed like a great approach to be used to study population dynamics, we purchased an Epson Perfection V800 Flatbed Photo Scanner scanner for future experiments. This scanner offered to scan at 6400 x 9600 dpi which gave us a resolution of 3 μm without magnification, which can be used to see individual snowflakes (see figure A.3).

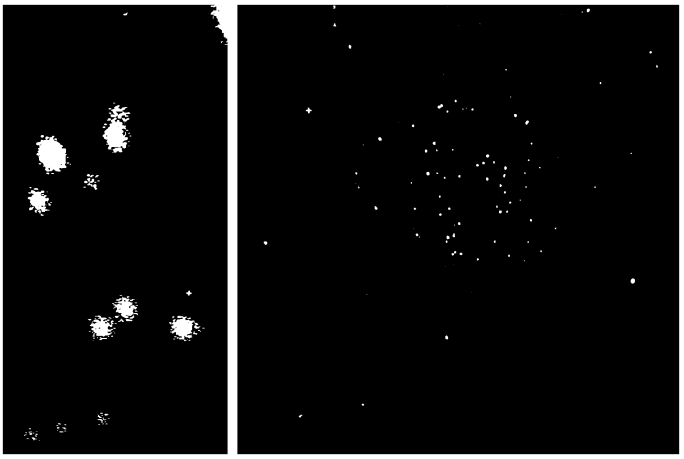

Figure A.3: Images of Snowflake using Epson V800 Scanner

In my opinion, scanner-based technologies have a lot to contribute to the field of quantitative biology for high-throughput data acquisition.

Appendix B

Fabrication of Microfluidic devices

Microfluidic devices are miniaturized experimental setups composed of micro-channels fabricated on glass, silicon or plastics like PDMS (poly-dimethylsiloxane)). The design and combinations of micro-channels can be altered to create valves, pressure-controlled pumps and controlled environments for biochemical reactions. Different sections of the microfluidic setup can have varying functionalities, whereby one can design a whole experiment, from preparation to measurement on a single slide making it a "lab-on-chip" device.

B.1 Developing master mold on Silicon Wafer

This procedure needs to performed in a cleanroom to avoid contamination by any source of dust. We performed this step in the Microfluidic Facility operated in NCBS, Bangalore.

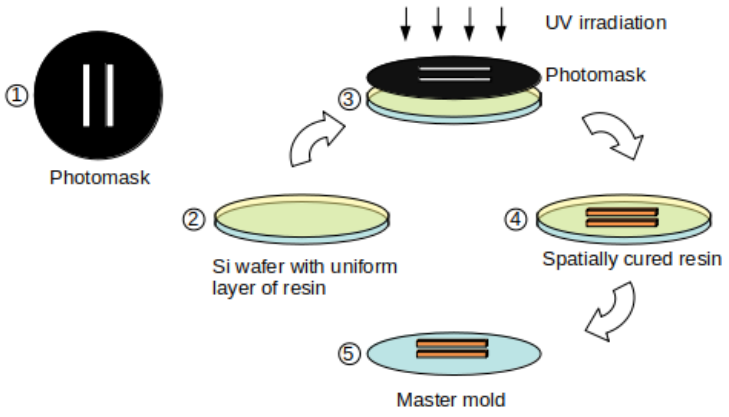

Figure B.1: Schema to develop master mold

Step 1: We begin with a Photo-lithography mask, an opaque plastic film with transparent regions in the design of our desired micro-channels. This design will determine the lengths and widths of our microfluidic device.

Step 2: We then cleaned a Si wafer and deposited a uniform layer of resin (SU-8) using a spin-coater. The thickness of the resin will determine the height of our micro-channels. We then soft bake the wafer with the resin on a heating plate.

Step 3: We placed the photo-lithography mask on top of the resin and exposed the wafer to UV light.

Step 4: The resin under the transparent region of the photo-lithography mask gets cured and hardens.

Step 5: We then develop the device with a solvent that etched away from the uncured regions. We end up with our micro-channels on top of the Si wafer.

Step 6: Finally, bake the Si wafer with our micro-channels on a heating plate one last time. The Si wafer is then stored in a closed petri dish.

B.2 Molding PDMS devices on glass substrate

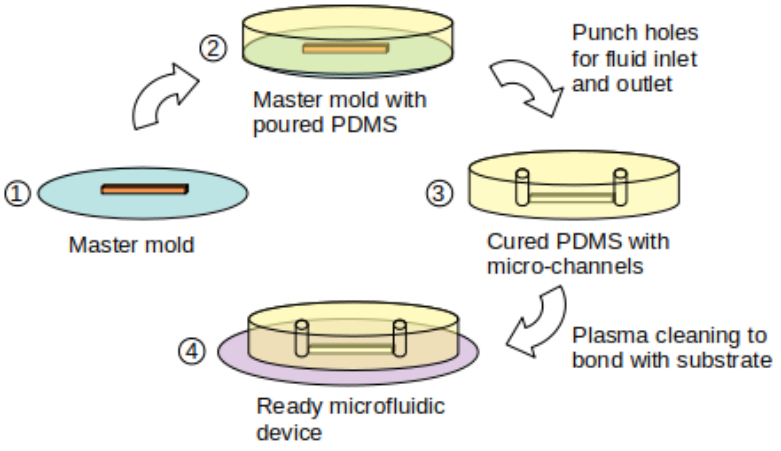

Figure B.2: Schema for moulding PDMS microfluidic devices

Step 1: We start with the master mould placed in a petri dish, prepared using the procedure mentioned above.

Step 2: We pour a solution of PDMS thoroughly mixed with a cross-linking agent onto the master mould and let it cure at 80^0C.

Step 3: We remove the hardened PDMS with imprinted micro-channels from the master mould and drill holes into it using a PDMS puncher.

Step 4: We plasma clean the PDMS mould along with a glass coverslip.

Step 5: Finally, we bond the PDMS mould onto the glass coverslip to make our microfluidic device.

B.3 Different functions of microfluidic devices

Once a master mould has been fabricated, it can be reused to make numerous devices. Depending on the photo-lithography mask, we can design devices to serve various functions (see figure B.3):

- To make droplet with various biochemical contents.
- Chambers to store droplets
- Channels to track flow of yeast cells etc

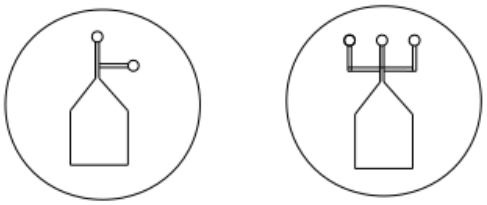

Figure B.3: Examples of Microfluidic devices

Bibliography

[1] Flow-cytometer schematic diagram kernel description. https://www.flowcytometrynet.com/flow-cytometers?lightbox=image_1dwl.

[2] Isothermal titration calorimeter schematic diagram kernel description. https://en.wikipedia.org/wiki/Isothermal_titration_calorimetry#/media/File:ITC1.png.

[3] T Bauchop and SR Elsden. The growth of micro-organisms in relation to their energy supply. *Microbiology*, 23(3):457–469, 1960.

[4] L. Boitard, D. Cottinet, C. Kleinschmitt, N. Bremond, J. Baudry, G. Yvert, and J. Bibette. Monitoring single-cell bioenergetics via the coarsening of emulsion droplets. *Proceedings of the National Academy of Sciences*, 109(19):7181–7186, 2012.

[5] Folmer Bokma. Evidence against universal metabolic allometry. *Functional Ecology*, 18(2):184–187, 2004.

[6] SRCP Brody, RC Procter, et al. Relation between basal metabolism and mature body-weight in different species of mammals and birds. *Relation between basal metabolism and mature body-weight in different species of mammals and birds.*, 1932.

[7] James H Brown, James F Gillooly, Andrew P Allen, Van M Savage, and Geoffrey B West. Toward a metabolic theory of ecology. *Ecology*, 85(7):1771–1789, 2004.

[8] Andrea K Bryan, Alexi Goranov, Angelika Amon, and Scott R Manalis. Measurement of mass, density, and volume during the cell cycle of yeast. *Proceedings of the National Academy of Sciences*, 107(3):999–1004, 2010.

[9] Scott C Burgess, Will H Ryan, Neil W Blackstone, Peter J Edmunds, Mia O Hoogenboom, Don R Levitan, and Janie L Wulff. Metabolic scaling in modular animals. *Invertebrate Biology*, 136(4):456–472, 2017.

[10] WA Calder. Size, function and life history. har, 1984.

[11] Mark Canciani, Argyris Arnellos, and Alvaro Moreno. Revising the superorganism: An organizational approach to complex eusociality. *Frontiers in Psychology*, 10, 2019.

[12] Pharmacia Fine Chemicals. *Percoll: Methodology and Applications: Density Marker Beads: for Calibration of Gradients of Percoll*. Pharmacia Fine Chemicals, 1980.

[13] Runar Collander. The permeability of nitella cells to rapidly penetrating non-electrolytes. *Physiologia Plantarum*, 3(1):45–57, 1950.

[14] Thomas H Dawson. Allometric relations and scaling laws for the cardiovascular system of mammals. *Systems*, 2(2):168–185, 2014.

[15] Peter Sheridan Dodds, Daniel H Rothman, and Joshua S Weitz. Re-examination of the "3/4-law" of metabolism. *Journal of Theoretical Biology*, 209(1):9–27, 2001.

[16] AL Does and LINDA F Bisson. Comparison of glucose uptake kinetics in different yeasts. *Journal of bacteriology*, 171(3):1303–1308, 1989.

[17] Andrew L Feig. Applications of isothermal titration calorimetry in rna biochemistry and biophysics. *Biopolymers: Original Research on Biomolecules*, 87(5-6):293–301, 2007.

[18] Douglas S Glazier. A unifying explanation for diverse metabolic scaling in animals and plants. *Biological Reviews*, 85(1):111–138, 2010.

[19] Douglas S Glazier. Rediscovering and reviving old observations and explanations of metabolic scaling in living systems. *Systems*, 6(1):4, 2018.

[20] Zoltán Göröcs, Yuye Ling, Meng Dai Yu, Dimitri Karahalios, Kian Mogharabi, Kenny Lu, Qingshan Wei, and Aydogan Ozcan. Giga-pixel fluorescent imaging over an ultra-large field-of-view using a flatbed scanner. *Lab on a Chip*, 13(22):4460–4466, 2013.

[21] Samir A Haddad and Carl C Lindegren. A method for determining the weight of an individual yeast cell. *Applied microbiology*, 1(3):153, 1953.

[22] Jon F Harrison. Do performance–safety tradeoffs cause hypometric metabolic scaling in animals? *Trends in ecology & evolution*, 32(9):653–664, 2017.

[23] Ira Herskowitz. Life cycle of the budding yeast saccharomyces cerevisiae. *Microbiological reviews*, 52(4):536, 1988.

[24] Shane Jacobeen, Elyes C Graba, Colin G Brandys, Thomas C Day, William C Ratcliff, and Peter J Yunker. Geometry, packing, and evolutionary paths to increased multicellular size. *Physical Review E*, 97(5):050401, 2018.

[25] Shane Jacobeen, Jennifer T Pentz, Elyes C Graba, Colin G Brandys, William C Ratcliff, and Peter J Yunker. Cellular packing, mechanical stress and the evolution of multicellularity. *Nature physics*, 14(3):286–290, 2018.

[26] Karl J Kaiyala and Douglas S Ramsay. Direct animal calorimetry, the underused gold standard for quantifying the fire of life. *Comparative Biochemistry and Physiology Part A: Molecular & Integrative Physiology*, 158(3):252–264, 2011.

[27] O Kestner. Metabolism and size of organs. *J. Physiol*, 87:39P–41P, 1936.

[28] M Kleiber. Body size and metabolism. hilgardia 6: 315-353.. 1961. the fire of life. *New York: Wiley.: 1972a. Body size, conductance for animal heat flow and Newton's law of cooling. J. Theoret. Biol*, 37:139–150, 1932.

[29] M Kleiber. The fire of life new york, 1961.

[30] Bogdan Łabedź, Aleksandra Wańczyk, and Zenon Rajfur. Precise mass determination of single cell with cantilever-based microbiosensor system. *PloS one*, 12(11), 2017.

[31] A Lavoie, J-L Mouget, and J de la Noile. Measurement of freshwater micro-algal cell density with percoll density gradients. *Journal of microbiological methods*, 4(5-6):251–259, 1986.

[32] Eric Libby, William Ratcliff, Michael Travisano, and Ben Kerr. Geometry shapes evolution of early multicellularity. *PLoS computational biology*, 10(9), 2014.

[33] P Peters. Ecological implication of body size. cambridge, mass.: Harvard univ. press. 331 p. 1983.

[34] Giorgio Pochetti and Roberta Montanari. Isothermal titration calorimetry to determine the association constants for a ligand bound simultaneously to two specific protein binding sites with different affinities. *Nature Protocol Exchange*, 2012.

[35] Cold Spring Harbor Laboratory Press. Yeast extract–peptone–dextrose (ypd) medium recipe. `http://cshprotocols.cshlp.org/content/2017/8/pdb.rec090563.full?text_only=true`, 2017.

[36] Md Habibur Rahman, Mohd Ridzuan Ahmad, Masaru Takeuchi, Masahiro Nakajima, Yasuhisa Hasegawa, and Toshio Fukuda. Single cell mass measurement using drag force inside lab-on-chip microfluidics system. *IEEE transactions on nanobioscience*, 14(8):927–934, 2015.

[37] William C Ratcliff, R Ford Denison, Mark Borrello, and Michael Travisano. Experimental evolution of multicellularity. *Proceedings of the National Academy of Sciences*, 109(5):1595–1600, 2012.

[38] William C Ratcliff, Johnathon D Fankhauser, David W Rogers, Duncan Greig, and Michael Travisano. Origins of multicellular evolvability in snowflake yeast. *Nature communications*, 6(1):1–9, 2015.

[39] Hans Ulrik Riisgård. No foundation of a'3/4 power scaling law'for respiration in biology. *Ecology Letters*, 1:71–73, 1998.

[40] Daniel Riveline and Paul Nurse. 'injecting'yeast. *Nature methods*, 6(7):513, 2009.

[41] Jonathan Rodenfels, Karla M Neugebauer, and Jonathon Howard. Heat oscillations driven by the embryonic cell cycle reveal the energetic costs of signaling. *Developmental cell*, 48(5):646–658, 2019.

[42] F Sarrus and JF Rameaux. Application des sciences accessoires et principalement des mathématiques à la physiologie générale (rapport sur une mémoire adressé à l'académic royale de médecine, séance du 23 juillet 1839). *Bull. Acad. R. Méd.(Paris)*, 3:1094–1100, 1839.

[43] Van M Savage, James F Gillooly, William H Woodruff, Geoffrey B West, Andrew P Allen, Brian J Enquist, and James H Brown. The predominance of quarter-power scaling in biology. *Functional Ecology*, 18(2):257–282, 2004.

[44] Albert Thommen, Steffen Werner, Olga Frank, Jenny Philipp, Oskar Knittelfelder, Yihui Quek, Karim Fahmy, Andrej Shevchenko, Benjamin M Friedrich, Frank Jülicher, et al. Body size-dependent energy storage causes kleiber's law scaling of the metabolic rate in planarians. *Elife*, 8:e38187, 2019.

[45] R Michael Van Dam. *Solvent-resistant elastomeric microfluidic devices and applications*. PhD thesis, California Institute of Technology, 2006.

[46] Geoffrey B. West, James H. Brown, and Brian J. Enquist. A general model for the origin of allometric scaling laws in biology. *Science*, 276(5309):122–126, 1997.

[47] Craig R White and Michael R Kearney. Metabolic scaling in animals: methods, empirical results, and theoretical explanations. *Comprehensive Physiology*, 4(1):231–256, 2011.

[48] Craig R White and Roger S Seymour. Mammalian basal metabolic rate is proportional to body mass2/3. *Proceedings of the National Academy of Sciences*, 100(7):4046–4049, 2003.

[49] Yanhua Wu, Dong Sun, and Wenhao Huang. Mechanical force characterization in manipulating live cells with optical tweezers. *Journal of biomechanics*, 44(4):741–746, 2011.

[50] Guoan Zheng, Xiaoze Ou, and Changhuei Yang. 0.5 gigapixel microscopy using a flatbed scanner. *Biomed. Opt. Express*, 5(1):1–8, Jan 2014.